U.S. Department
of Transportation
Federal Railroad
Administration

Office of Research,
Development and Technology
Washington, DC 20590

High-Strength, Reduced-Modulus, High-Performance Concrete for Prestressed Concrete Crosstie Applications

REPORT DOCUMENTATION PAGE

Form Approved
OMB No. 0704-0188

1. AGENCY USE ONLY (Leave blank)	2. REPORT DATE	3. REPORT TYPE AND DATES COVERED
	May 2021	Technical Report

4. TITLE AND SUBTITLE
High-Strength, Reduced-Modulus, High-Performance Concrete for Prestressed Concrete Crosstie Applications

5. FUNDING NUMBERS
DTFR5314C00023

6. AUTHOR(S) Dimitris C. Rizos, Ph.D., Adam Zeitouni, Ali Abdulqader

7. PERFORMING ORGANIZATION NAME(S) AND ADDRESS(ES)
University of South Carolina
Columbia, South Carolina 29208

8. PERFORMING ORGANIZATION REPORT NUMBER

9. SPONSORING/MONITORING AGENCY NAME(S) AND ADDRESS(ES)
U.S. Department of Transportation
Federal Railroad Administration
Office of Railroad Policy and Development
Office of Research, Development, and Technology
Washington, DC 20590

10. SPONSORING/MONITORING AGENCY REPORT NUMBER
DOT/FRA/ORD-23/26

11. SUPPLEMENTARY NOTES
COR: Cameron Stuart

12a. DISTRIBUTION/AVAILABILITY STATEMENT
This document is available to the public through the FRA eLibrary.

12b. DISTRIBUTION CODE

13. ABSTRACT (Maximum 200 words)

High-performance concrete (HPC) with early strength development is the material of choice for fabricating prestressed concrete railroad ties. However, the higher strength of HPC results in significantly higher elastic modulus values and increases the rigidity of the tie, leading to higher amplitude stresses and stress gradients, and eventually to premature cracking and deterioration of the railroad ties. This report presents material development and characterization studies of high-strength, reduced-modulus (HSRM) concrete and its application for concrete railroad ties. Prototype ties have been fabricated and qualified through testing and computer simulations. The fabrication of the HSRM ties did not affect the current fabrication practices and cost. This study shows that HSRM ties outperformed standard concrete ties by (a) showing smoother stress distribution, (b) delaying the initiation of cracks, (c) redistributing the load after first cracking in an effective manner, and (d) failing at higher ultimate loads. Researchers suggest HSRM concrete is a cost-effective alternative concrete to the industry standard concrete used in ties and has the potential to increase its tie service life.

14. SUBJECT TERMS
Concrete, crosstie, weathered aggregate, granite, modulus

15. NUMBER OF PAGES
55

16. PRICE CODE

17. SECURITY CLASSIFICATION OF REPORT	18. SECURITY CLASSIFICATION OF THIS PAGE	19. SECURITY CLASSIFICATION OF ABSTRACT	20. LIMITATION OF ABSTRACT
Unclassified	Unclassified	Unclassified	

NSN 7540-01-280-5500
Standard Form 298 (Rev. 2-89)
Prescribed by ANSI Std. 239-18
298-102

METRIC/ENGLISH CONVERSION FACTORS

ENGLISH TO METRIC	METRIC TO ENGLISH
LENGTH (APPROXIMATE)	**LENGTH (APPROXIMATE)**
1 inch (in) = 2.5 centimeters (cm)	1 millimeter (mm) = 0.04 inch (in)
1 foot (ft) = 30 centimeters (cm)	1 centimeter (cm) = 0.4 inch (in)
1 yard (yd) = 0.9 meter (m)	1 meter (m) = 3.3 feet (ft)
1 mile (mi) = 1.6 kilometers (km)	1 meter (m) = 1.1 yards (yd)
	1 kilometer (km) = 0.6 mile (mi)
AREA (APPROXIMATE)	**AREA (APPROXIMATE)**
1 square inch (sq in, in^2) = 6.5 square centimeters (cm^2)	1 square centimeter (cm^2) = 0.16 square inch (sq in, in^2)
1 square foot (sq ft, ft^2) = 0.09 square meter (m^2)	1 square meter (m^2) = 1.2 square yards (sq yd, yd^2)
1 square yard (sq yd, yd^2) = 0.8 square meter (m^2)	1 square kilometer (km^2) = 0.4 square mile (sq mi, mi^2)
1 square mile (sq mi, mi^2) = 2.6 square kilometers (km^2)	10,000 square meters (m^2) = 1 hectare (ha) = 2.5 acres
1 acre = 0.4 hectare (he) = 4,000 square meters (m^2)	
MASS - WEIGHT (APPROXIMATE)	**MASS - WEIGHT (APPROXIMATE)**
1 ounce (oz) = 28 grams (gm)	1 gram (gm) = 0.036 ounce (oz)
1 pound (lb) = 0.45 kilogram (kg)	1 kilogram (kg) = 2.2 pounds (lb)
1 short ton = 2,000 pounds (lb) = 0.9 tonne (t)	1 tonne (t) = 1,000 kilograms (kg) = 1.1 short tons
VOLUME (APPROXIMATE)	**VOLUME (APPROXIMATE)**
1 teaspoon (tsp) = 5 milliliters (ml)	1 milliliter (ml) = 0.03 fluid ounce (fl oz)
1 tablespoon (tbsp) = 15 milliliters (ml)	1 liter (l) = 2.1 pints (pt)
1 fluid ounce (fl oz) = 30 milliliters (ml)	1 liter (l) = 1.06 quarts (qt)
1 cup (c) = 0.24 liter (l)	1 liter (l) = 0.26 gallon (gal)
1 pint (pt) = 0.47 liter (l)	
1 quart (qt) = 0.96 liter (l)	
1 gallon (gal) = 3.8 liters (l)	
1 cubic foot (cu ft, ft^3) = 0.03 cubic meter (m^3)	1 cubic meter (m^3) = 36 cubic feet (cu ft, ft^3)
1 cubic yard (cu yd, yd^3) = 0.76 cubic meter (m^3)	1 cubic meter (m^3) = 1.3 cubic yards (cu yd, yd^3)
TEMPERATURE (EXACT)	**TEMPERATURE (EXACT)**
[(x-32)(5/9)] °F = y °C	[(9/5) y + 32] °C = x °F

QUICK INCH - CENTIMETER LENGTH CONVERSION

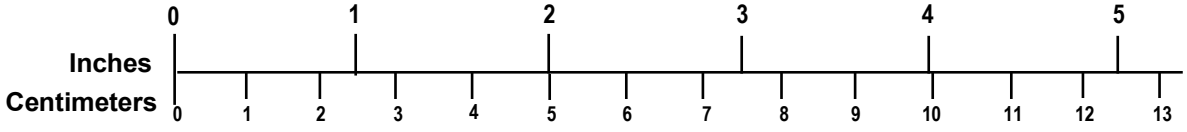

QUICK FAHRENHEIT - CELSIUS TEMPERATURE CONVERSIO

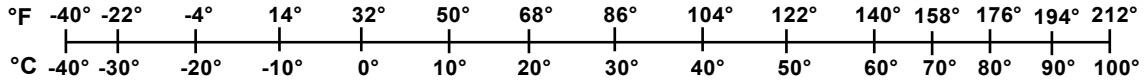

For more exact and or other conversion factors, see NIST Miscellaneous Publication 286, Units of Weights and Measures. Price $2.50 SD Catalog No. C13 10286

Updated 6/17/98

Acknowledgments

The authors acknowledge the support and contributions of CSX Transportation and KSA (now ROCLA Concrete Tie). The support and insight provided by Cameron Stuart, John West, Tod Echler, Ryan Rolfe, Scott Craig, and Hailing Yu is greatly appreciated. The authors extend their appreciation to Professor Michael Sutton at the University of South Carolina for his guidance with the StereoDIC system and Sreehari Katil, Russell Inglett, Tim Ross, Josh Breed, Melissa Brueckner, and Brigitte Shumpert for their assistance with laboratory and plant activities.

Contents

Illustrations

Tables

Executive Summary

Researchers at the University of South Carolina developed a high-strength concrete with a modulus of elasticity significantly lower than industry standard designs and tested this new material for use in railroad concrete crossties. The research team qualified high-strength, reduced-modulus (HSRM) ties according to the AREMA Manual for Railway Engineering guidelines and demonstrated their benefits through laboratory testing and computer simulation studies. This research was sponsored by Federal Railroad Administration and conducted between August 2014 and July 2018. This project utilized university laboratory facilities for modeling and testing, produced prototype concrete ties at the KSA (now Rocla Concrete Tie) manufacturing plant, and relied upon CSX Transportation technical support throughout the period of performance.

This research demonstrates the use of HSRM in prestressed concrete ties to address critical issues that affect the service life of standard concrete ties. Specifically, this project shows that ties made with HSRM concrete have the same high strength as with standard concrete designs but are significantly more flexible, allowing for better load distribution in the tie and the track, thus preventing premature cracking.

The investigations were conducted in three phases: (a) material development and characterization, (b) prototype fabrication and product qualification, and (c) performance assessment and benefits.

The research team's findings include:

- The HSRM concrete compressive strength was comparable to the standard mix.
- The HSRM modulus of elasticity was lower than the standard mix, by as much as 50 percent.
- HSRM concrete had a much higher abrasion resistance than the standard concrete.
- HSRM ties met the AREMA performance requirements and equaled or exceeded the performance of the standard ties.
- HSRM ties exhibited smoother stress gradients and exhibited stress redistribution after initial cracking.
- HSRM ties have lower stress amplitudes compared to standard ties under the same loads
- HSRM ties withstood higher ultimate loads.
- The use of weathered granites to produce the HSRM concrete ties did not impact the production process or increase the cost of the ties.

The use of HSRM represents a technology-based modification in concrete tie manufacturing that improves the safety of rail service and maintenance operations without impacting fabrication cost and process. This study suggests that the HSRM concrete may become a cost-effective alternative to the traditional high-performance concrete used in prestressed concrete ties with the potential to increase the service life of the tie.

Testing the in-track performance of HSRM ties under service operating conditions is recommended. Future work will also include tie design optimization based on HSRM material, investigations on the use of HSRM concrete in other concrete tie designs and systems, as well as its use in other railroad infrastructure parts.

1. Introduction

Researchers at the University of South Carolina developed a high-strength concrete with a modulus of elasticity significantly lower than industry standard designs and tested this new material for use in railroad concrete crossties. This research was sponsored by Federal Railroad Administration and conducted between August 2014 and July 2018. This project utilized university laboratory facilities for modeling and testing, produced prototype concrete ties at the KSA (now Rocla Concrete Tie) manufacturing plant, and relied upon CSX Transportation technical support throughout the period of performance. This introductory section presents the background information, motivation, and objectives related to this work. It also discusses the scope of work and the approach used to achieve the objectives.

1.1 Background

Crossties are one of the main structural components of railroad track, supporting the rails and distributing train axle loads to the ballast. Prestressed concrete ties have become an alternative to traditional timber ties for freight, passenger, and transit lines due to their increased strength, stability, and durability characteristics (Weart, 2008). Concrete ties must have a longer service life and require less maintenance compared to timber ties to offset their higher initial costs. High-strength (HS) concrete with early strength development is currently the material of choice in the fabrication of prestressed concrete railroad ties; they have a design life of over 50 years (Lutch, Harris, & Ahlborn, 2009).

However, concrete ties often do not reach their design life due to several unresolved performance issues (Kaewunruen & Remennikov, 2010; Jeong & Yu, 2012). Frequent inspections of many railroad tracks have uncovered concrete ties that have prematurely failed or cracked well before their designed service life. A 2010 study sponsored by the Railway Tie Association reported that of the "29 million ties that were installed since the 1970s, approximately 2.2 to 2.7 million ties were reported as failed and replaced" (ZETA-TECH, 2010). That is an approximate failure rate of 7.9 to 9.2 percent. These unexpected findings have prompted the need for further field investigations to assess the performance and behavior of concrete ties in service.

In 2014, the Federal Railroad Administration (FRA) studied the performance of concrete ties that were installed on the Northeast Corridor (NEC) to determine the factors that lead to early cracking (FRA, 2014). The authors sought to study the horizontal cracking phenomenon known to appear along the top row of prestressed steel tendons located at one or both ends of a tie. The authors sampled different concrete ties of varying age and from five separate locations along Amtrak NEC lines. The concrete ties were inspected in both the field and laboratory. The concrete ties in the field were examined visually and non-destructively by the impact echo method. Laboratory tests were performed for modulus and strength, tensile strength, and flexural strength data, among others. Furthermore, the authors simulated various tests on the concrete ties by conducting finite element analysis.

Based on the results from the FRA study's extensive examinations, the authors concluded that the premature cracking of the concrete ties was caused by a combination of contributing factors. The first was a high concentration of tensile stress in the concrete ties, primarily located at the location of the prestressing steel, which is caused by the transfer of forces when the prestressed strands are released. The second factor was associated with the pressures produced by an alkali-

silica reaction (ASR) that caused excessive internal stresses. Additionally, the authors concluded that other factors, such as cyclic freezing and thawing, delayed ettringite formation, and stresses due to fastener inserts or unusual tie vibrations were not major contributors to premature cracking of these specific ties.

Longitudinal cracking is not the only concern related to the premature failure of concrete ties. Zeman (2010), for example, published an extensive study on the rail seat deterioration (RSD) of concrete ties. Manda and his co-authors studied the effect of static and dynamic loads on the tie and fastening system (Manda, Dersch, Edwards, & Lange, 2014). Surveys among the North American railroad companies (Zeman, Edwards, Barkan, & Lange, 2009; Van Dyk, Dersch, & Edwards, 2016) have shown that the most critical issues in tie performance, in order of importance, are: (1) RSD; (2) shoulder/fastener wear or fatigue; (3) derailment damage; (4) cracking from center binding; (5) cracking from dynamic loads; and (6) tamping damage, among others. The primary causes of RSD appear to be high stresses at the rail seat, a loosened fastening system, the presence of moisture, and the presence of abrasive fines. Cracking from center binding and dynamic loads is due to the development of high tensile stresses. Therefore, the development of high-amplitude stresses and the corresponding stress distribution within the tie appears to be a common underlying cause of the most critical issues that affect tie performance. In turn, high stresses and stress distribution are directly related to a combination of the strength and stiffness of a tie. Typically, a high-strength but relatively flexible load-bearing element results in more regularized (smoother) stress field gradients with reduced amplitudes that should alleviate the issues associated with high stresses in concrete ties. However, for a given tie geometry, strength and stiffness depend on the strength and elastic modulus of the materials. The higher strength of high-performance concrete (HPC) is directly related to higher values of the elastic modulus, thus increasing the rigidity of the material. Consequently, the combination of increased strength, rigidity, and brittleness may lead to premature cracking and deterioration of the concrete ties.

Research conducted in 2000 (Petrou, Rizos, Harries, & Hanson, 2004) revealed that HPC mixtures could be classified as U.S. Federal Highway Administration (FHWA) Grade 1 or 2, based on their durability and strength properties (Goodspeed, Venikar, & Cook, 1996). In the process of the 2000 study, it was incidentally discovered that the values obtained for the modulus of elasticity for several the design mixes were well below the range of values specified for Grade 1 of the FHWA classification. In addition, the elastic modulus of concrete could not be predicted using any of the empirical equations (e.g., ACI, 2014; ACI Committee 363, 1992; BSCP, 1972). An extensive investigation concluded that the low modulus values are attributable to the degree of weathering observed in the granite aggregates. These weathered granite aggregates can be found in South Carolina; (Aitkin & Mehta, 1990; Alexander & Milne, 1995; Giaccio, Rocco, Violini, Zappitelli, & Zerbino, 1992; Wu, Ke-Ru, Bing, & Dong, 2001).

The major conclusions of the preceding work have been summarized by Petrou, Rizos, Harries, and Hanson (2004):

> (1) The modulus of elasticity of HPC is significantly affected by the extent of weathering on crushed granite aggregate and the susceptibility of its source to the weathering process, as shown in Figure 1 (a). Weathered aggregates should not be used in HPC mixes for bridge construction.

(2) For unaltered granite aggregate concrete, as the concrete compressive strength increases so does the elastic moduli of the associated HPC. For weathered aggregate concrete, there is little correlation between the concrete elastic modulus and its compressive strength, as shown in Figure 1 (b).

(3) The design code equations may overestimate the elastic modulus of concrete with weathered aggregates by as much as 70 percent.

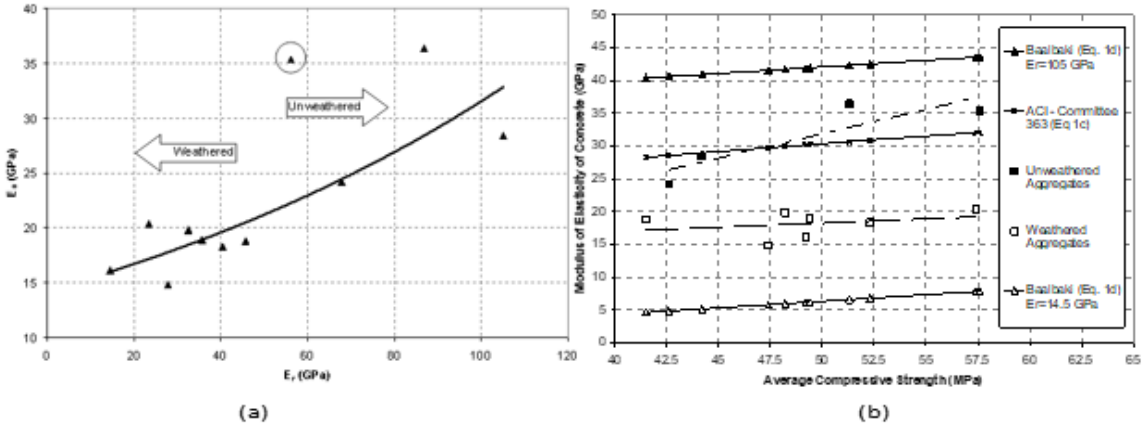

Figure 1. Correlations of modulus of elasticity of HPC with weathered and unweathered aggregates with (a) modulus of elasticity of rock material and (b) average compressive strength (Petrou, Rizos, Harries, & Hanson, 2004)

1.2 Objectives

This work investigates the benefits of using high-strength, reduced-modulus (HSRM) concrete in place of the currently used high-strength (standard) concrete mixes in the fabrication of prestressed concrete rail ties. The hypothesis is that the use of HSRM in the fabrication of ties combines the advantages of the high strength of HPC while preserving the structural performance advantages of more flexible materials. Specifically, this work demonstrates that HSRM ties have the same or higher strength as the standard ties but are significantly more flexible, allowing for better load distribution in the tie and the track, smaller stress amplitudes, and a smoother stress gradient. This work demonstrates that premature failures can be avoided, and damage initiation delayed, thus extending the service life of the ties.

The objectives of this work are summarized as:

1. Develop and characterize a HSRM concrete consistent with the specifications for use in prestressed concrete ties.
2. Produce, test, and qualify a prototype prestressed concrete tie made of this HSRM concrete material.
3. Investigate the performance of HSRM and standard ties through physical testing and computer simulations.
4. Quantify the benefits of using HSRM concrete in place of standard concrete in prestressed concrete ties.

1.3 Overall Approach

To achieve the objectives set in Section 1.2, the research team studied a prestressed concrete tie design currently available in the U.S. market. The team adopted the design specifications of this standard tie in developing the HSRM material and the prototype HSRM tie. A series of physical tests and computer simulations compared the performance of the HSRM and standard ties. The standard tie provided the baseline data for quantifying the performance of the HSRM tie.

The investigation was conducted in three phases: (a) material development and characterization, (b) prototype fabrication and product qualification, and (c) performance assessment and benefits.

The first phase pertains to material development and characterization of the HSRM concrete using weathered granite aggregates from different sources. The HSRM concrete mix design was the same as the standard mix, with the exception that the HSRM used weathered granite as coarse aggregate in place of the limestone coarse aggregates used in the standard design. The gradation of the weathered granites was the same as the limestone coarse aggregate. The mechanical properties of the HSRM and standard concretes and the constituent materials were determined through ASTM standard testing. In addition to the ASTM standard tests, a lapping test was performed on the hardened concrete to measure the abrasion resistance of the concrete. This lapping test was developed by University of Illinois Urbana-Champaign (UIUC) (Van Dam, 2016).

The second phase focused on the fabrication of prototype HSRM ties and baseline standard ties. All ties were fabricated at the KSA concrete tie fabrication facility and shipped to the laboratories for testing and qualification. Qualification tests were conducted in accordance with AREMA guidelines for prestressed concrete tie testing.

The last phase quantified the benefits of using HSRM concrete in place of standard concrete through a comparison of the structural performance of each tie. Researchers conducted these studies through lab testing and computer simulations.

1.4 Scope

The scope of this work was to develop the HSRM material and establish its mechanical properties. This work adopted one commercially available tie design to demonstrate the benefits of using HSRM concrete through a direct comparison of the structural performance of HSRM and standard ties. The work reported here did not consider the optimization of tie design based on the HSRM material. In addition, this study did not consider other commercially available designs, including post-tensioning systems or any other concrete mix designs.

1.5 Organization of the Report

Section 2 introduces the geometry, material, and design parameters of the standard tie considered as the baseline in this study. Section 3 describes the development of the HSRM material and the determination of its mechanical properties. Section 4 discusses the production of prototype ties used in the qualification, testing, and evaluation tasks in this work. Section 5 introduces the testing setups and instrumentation used in the experimental tasks of this work, including the Stereo DIC data acquisition system and the tie qualification studies. Section 6 presents the experimental and analytical investigations conducted to establish the benefits of the HSRM ties and discusses the findings. A summary of the findings and recommendations for future work is presented in the Conclusion, Section 7.

2. The Baseline Prestressed Concrete Tie – "Standard" Tie

The tie design used in this study is based on a commercially available tie produced by a major U.S. tie manufacturer for a Class I railroad. This section presents the materials, geometry, design parameters, and nominal capacities of the standard tie.

2.1 Design Parameters

The length of the tie is 8 feet, 6 inches, and its detailed geometry is shown in Figure 2. Prestressing force is applied through eight, 7-wire, ASTM A886 Grade 270 low-relaxation strands, each 3/8 inch in diameter, placed in two rows.

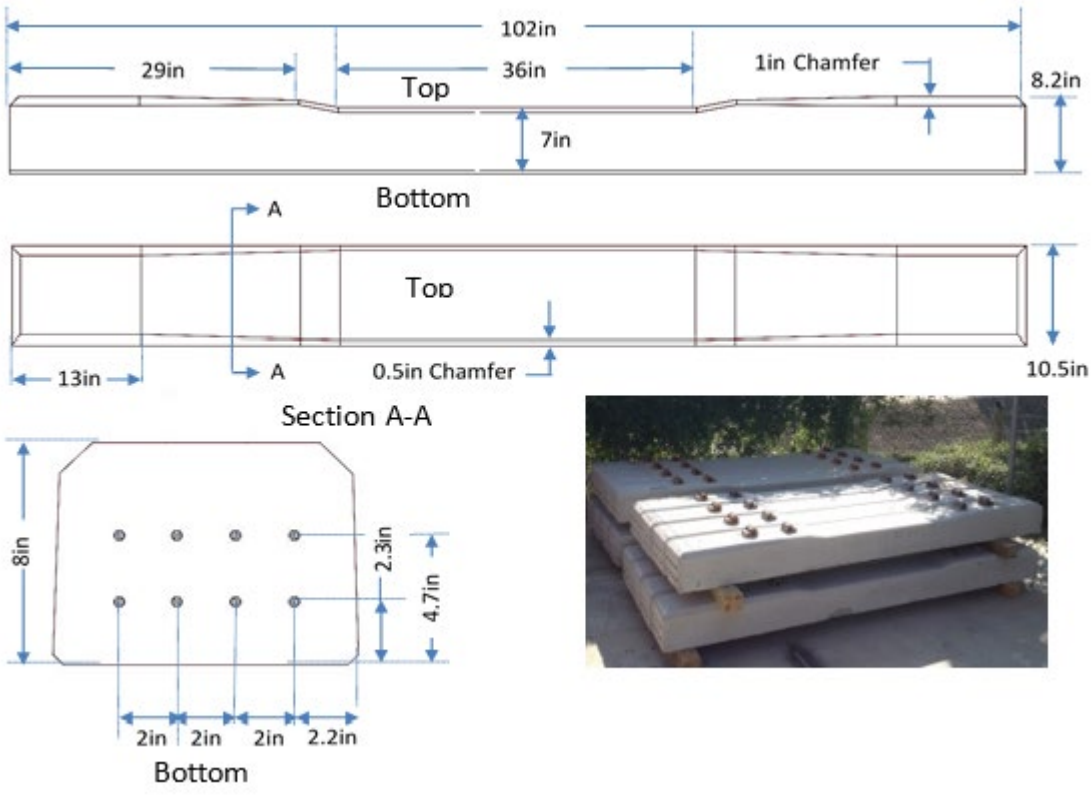

Figure 2. Geometric design drawings and manufactured ties

The baseline tie design parameters are listed in Table 1.

Table 1. Concrete tie design parameters

Description	Symbol	Value	
Area of tie at rail seat	A_{tr}	81.00	in^2
Area of tie at center	A_{tc}	71.5	in^2
Strand eccentricity at rail seat	e	0.45	in
Section modulus wrt to bottom of tie	S_B	108.5	in^4
Strand diameter	d_s	3/8	in

Description	Symbol	Value	
Strand area	A_s	0.11	in^2
Prestressing force per strand	P_i	17.25	kip
Effective force per strand	P_e	15.36	kip
Strand initial stress	σ_i	156.2	ksi
Effective strand stress	σ_{ie}	139	ksi
Number of strands	N_s	8	
Total prestressing force	P_{si}	138	kip
Total effective force	P_{se}	123	kip
Modulus of elasticity for steel	E_s	29,000	ksi

Assuming a standard sign convention for internal forces in a beam, and defining the "top" and "bottom" of the tie to be as shown in Figure 2, the nominal moment, associated stress, and corresponding force required to produce the design moment in qualification tests set forth in AREMA Manual for Railway Engineering Chapter 30, Section 4.9.1, at the top and bottom of the strand, is summarized in Table 2.

Table 2. Nominal capacity of railroad tie

	Rail Seat Center		Tie Center	
	Positive	Negative	Positive	Negative
Moment (in-kip)	300	162	144	208
Force[1] (kips)	51.1	28.2	10.4	15.0
Stress Top (ksi)	-3.79	0.69	-3.28	1.0
Stress Bottom (ksi)	0.94	-3.31	0.15	-4.03

[1] Force required to produce the design moment in qualification tests set forth in AREMA Manual for Railway Engineering Chapter 30 Section 4.9.1.

2.2 Concrete Mix Design

The tie manufacturer provided the concrete mix design for the standard tie. The manufacturer's mix design yields a concrete with a minimum 7 ksi compressive strength at 28 days. The standard concrete reaches a compressive strength of 4 ksi within 24 hours after pour to meet the strength demands for de-tensioning of the strands. Type III cement, conforming to ASTM C150, provides high early strength. Admixtures are used in the mix to increase the workability of the wet concrete and control the air entrainment during production. The concrete mix design is shown in Table 3.

Table 3. Concrete mix design

Material	Amount	Comments
Cement	600 lb/yd^3	ASTM C-150 Type III, low alkali (Speed, Indiana)
Water	234 lb/yd^3	City water
Coarse Aggregate	1,842 lb/yd^3	Plum Run Stone (size #67, ASTM C-33)
Sand	1,333 lb/yd^3	Plum Run Stone (ASTM C-33)
Micro Air	0.7 oz/cwt	Master Builders (ASTM C-260 Air Entraining Admixture)
Glenium	10 oz/cwt	Master Builders (ASTM C-494 Super)

3. HSRM Material Development and Characterization

This section presents the steps for developing the HSRM concrete material and summarizes the test results for identifying its mechanical properties.

3.1 Coarse Aggregates and the HSRM Design Mix

The reduction of the elastic modulus in concrete is achieved using weathered granites as the coarse aggregate. The researchers obtained crushed weathered granite from three quarries, hereafter identified as CA2, CA3, and CA4. Figure 3 shows the aggregate as delivered and samples of the CA2, CA3, and CA4 weathered granite aggregates. The HSRM concrete mix design was the same as the standard concrete mix design introduced in Section 2.2, with the exception that the coarse aggregates were replaced with the crushed weathered granite material by weight. The tie manufacturer delivered the plum run stone coarse aggregate that they use in the production of standard ties. The plum run stone is a limestone coarse aggregate and is hereafter identified as CA1. In addition, the tie manufacturer shipped the plum run stone sand for use in the standard and HSRM prototype tie fabrication.

Figure 3. Weathered granite coarse aggregates: (a) as delivered to USC laboratories, (b) CA2, (c) CA3, (d) CA4

3.2 Mechanical Properties

A series of tests were conducted on each of the aggregates and fresh and hardened concrete samples to determine commonly reported properties (Table 4). A second batch was produced and tested to verify the consistency. These results were within 3 percent of the first batch. In addition to the ASTM standard tests, UIUC developed lapping test was performed on the hardened concrete to measure the abrasion resistance of the concrete. The test is designed to simulate the abrasion mechanism causing RSD. The abrasion was measured as the rate of loss of material in mm/sec during testing; lower values indicate better performance. All specimen fabrication and testing activities were performed in the materials and structures laboratory at USC, except for the lapping test. This test was conducted at the Rail Transportation and Engineering Center (RailTEC) laboratory at UIUC.

Table 4. Properties of concrete produced with limestone and weathered granite coarse aggregates from 3 sources

Property	ASTM Test	Standard CA1-B1	HSRM CA2-B1	HSRM CA3-B1	HSRM CA4-B1
Aggregates					
Voids	C127	42.73	42.51	39.90	39.10
Density (lb/ft^3)	C29	161.65	164.50	165.00	167.50
LA Abrasion	C131	27.5%	33.9%	44.3%	46.0%
Fresh Concrete					
Density (lb/ft^3)	C138	152.90	153.73	154.14	158.55
Yield (yd^3)	C138	0.15	0.15	0.14	0.14
Cement Content (lb/yd^3)	-	618.23	621.53	623.21	632.05
Slump (in)	C143	7.00	6.50	7.50	4.00
Air Content (%)	C231	5.0%	5.9%	4.8%	4.0%
Hardened Concrete					
Compressive Strength (psi) 28-day	C39	8.8E+03	8.8E+3	9.2E+03	8.7E+03
Strength Increase/Reduction %		***0%***	***0%***	***4%***	***-1%***
Flexural Strength (psi) 28-day	C78	0.13fc'	0.12fc'	0.12fc'	-
Elastic Modulus (psi) 28-day	C469	5.6E+06	3.6E+06	3.2+06	2.8E+06
Elastic Modulus Reduction %		***0%***	***37%***	***43%***	***50%***
Lapping Test Abrasion Rate		0.042	0.023	0.029	0.039

Researchers observed that:

1. The voids and density of limestone and weathered granite aggregates were very similar; however, the LA abrasion test showed that weathered granite aggregate exhibited higher loss.
2. The fresh concrete properties were very similar for all concrete mixes.
3. The aggregate type did not affect the compressive and flexural strength of concrete.
4. The modulus of elasticity of concrete containing weathered granite coarse aggregate was significantly lower (up to 50 percent) than the standard concrete.
5. The lapping test showed superior performance of the HSRM concrete compared to standard concrete. This seemed contradictory to the LA abrasion test results on the aggregates. This was attributed to the different abrasion mechanisms between the two tests. The impact by the steel spheres in the LA abrasion test broke the structure of the partially weathered granite aggregate, causing the measured loss. However, once aggregate was confined in the cement matrix, the higher hardness of granites contributed to the better performance of the HSRM under grinding.

The graphs in Figure 4 (a) and (b) show the development of the compressive strength and modulus of elasticity for each batch with respect to time.

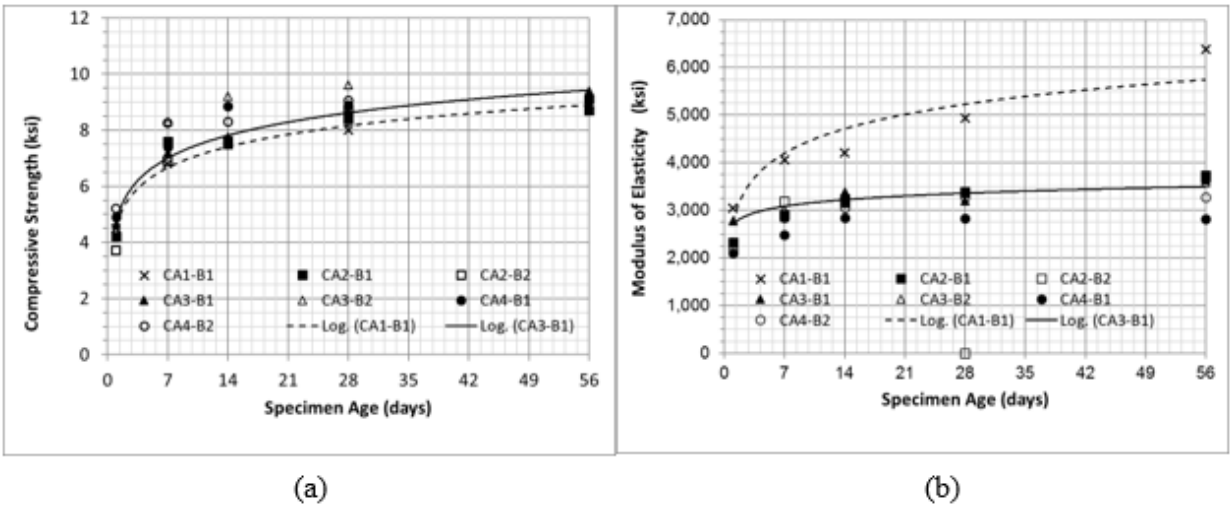

Figure 4. Comparison between HSRM and standard concrete: (a) compressive strength vs. specimen age and (b) modulus of elasticity vs. specimen age

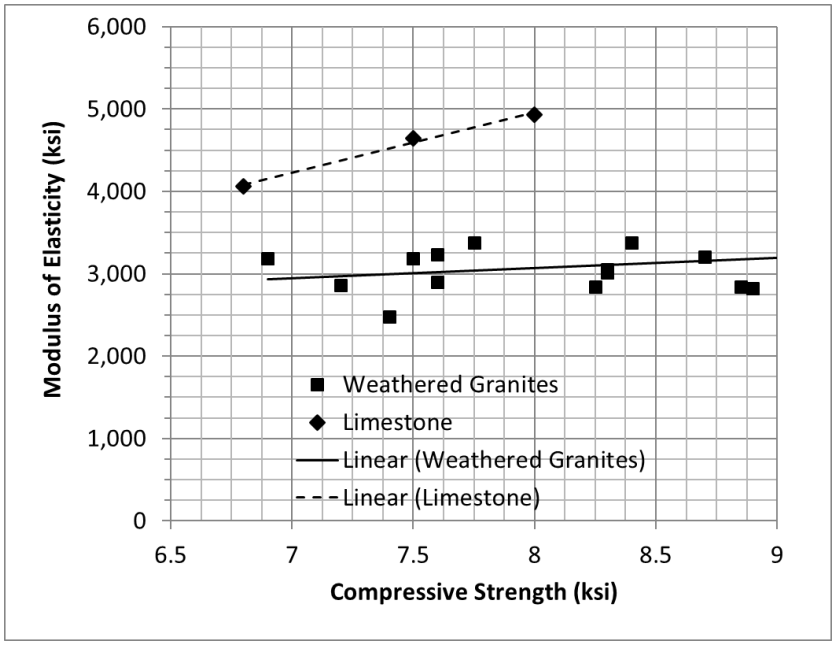

Figure 5. Correlation of modulus of elasticity with compressive strength for the HSRM (CA3-B%) and standard concrete (CA1-B5)

Researchers observed that the compressive strength developed as expected for both the HSRM and standard concrete, with the HSRM concrete exhibiting a compressive strength equal or greater than the standard concrete. However, the modulus of elasticity for the HSRM concrete appeared to plateau after its early strength was achieved, while the modulus of elasticity for the standard concrete continued to increase as its strength increased over time. The modulus reduction achieved by both plant batches was 20 to 30 percent at 14 days and 43 to 56 percent at 56 days. It was evident that there was a very weak correlation between the modulus of elasticity and compressive strength for the HSRM material, as shown in Figure 5.

3.3 Weather Aggregate Selection

In summary, the weathered granite aggregates from all three sources produced HSRM concretes that met or exceeded the material property requirements of the standard concrete specified in the tie design adopted in this study. In addition, all three aggregates produced HSRM concretes that exhibited the lower elastic modulus sought after in this research, and all three exhibited higher resistance to surface abrasion than the standard concrete. Therefore, all three materials were deemed appropriate to produce the prestressed concrete ties. However, due to limitations in the scope of work, just one aggregate was selected to produce the prototype tie for the product qualification and performance assessment tasks. CA2 produced the least reduction in the elastic modulus of concrete and may not demonstrate the full benefits of the technology. CA4 produced the greatest reduction of the elastic modulus of concrete, but with a slightly lower compressive strength. Aggregate CA3 produced the highest strength concrete with a reduction in elastic modulus that was comparable, though slightly higher, to CA4. In addition, the CA3 concrete showed a higher resistance to surface abrasion than CA4 and had fresh concrete properties that compared better to the standard concrete. Therefore, CA3 was chosen to produce the prototype ties.

4. Prototype Tie Fabrication and Qualification

Standard and prototype (HSRM) concrete ties were produced at the same time and in the same prestressing bed at a major tie manufacturer plant on two different dates, approximately 12 months apart. In this plant, the freshly mixed concrete was poured into a pre-stressing bed, which consisted of 37 steel cavities arranged in series. Each cavity contained eight steel tie forms and was enclosed on both ends by removable steel plates. The steel strands ran continuously throughout the length of the bed, eight strands per steel form. Before the placing the concrete, the strands were pre-tensioned, with an initial force of 17.25 kips, by a hydraulic system at one end of the bed. On the other end of the bed, the steel stands were anchored on a bulkhead. For simplicity, the bed end containing the hydraulic system was designated the "live end," and the bed end anchoring the strands is the "dead end."

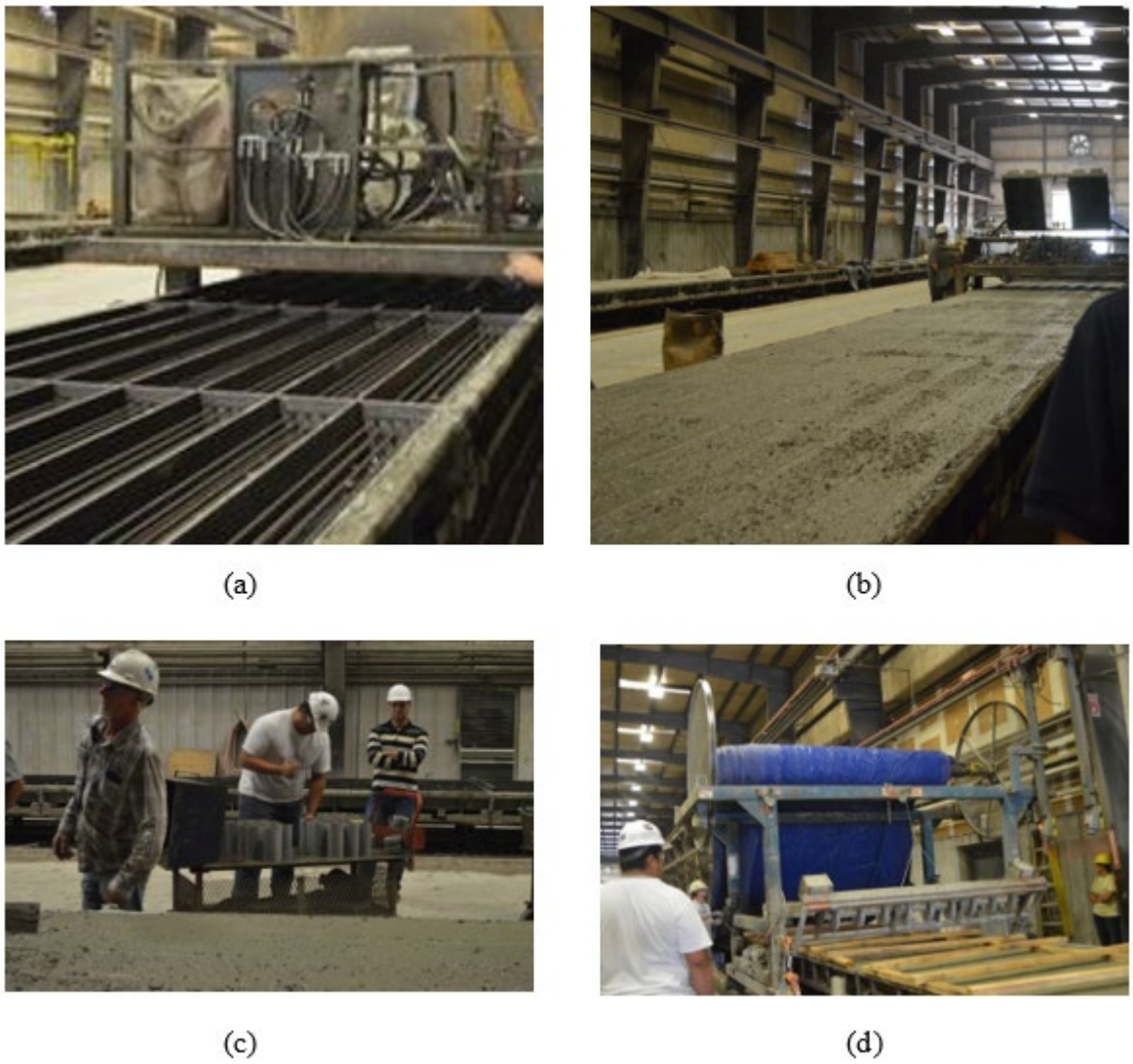

Figure 6. Concrete tie prestressing bed: (a) before placement of concrete; (b) after placement of concrete; (c) concrete cylinder preparation and (d) covering bed in preparation of concrete curing

The plant produced 32 prototype HSRM ties with aggregate CA3, and 32 standard ties with aggregate CA1 over 2 days of production. The first five cavities from the live end were used for HSRM tie production. The manufacturer shipped the 64 ties to the Structural Testing Laboratory at USC approximately 3 months after fabrication.

4.1 Material Properties

The HSRM concrete batches were identified as CA3-B5 and CA3-B7 and the standard concrete batches as CA1-B5 and CA1-B7, with batches B5 and B7 corresponding to the first and second production dates, respectively. The graphs in Figure 7 (a) and (b) show the development of the compressive strength and modulus of elasticity for each batch with respect to time. The concrete batches produced in the laboratory, CA1-B1 and CA3-B1, are also plotted for reference.

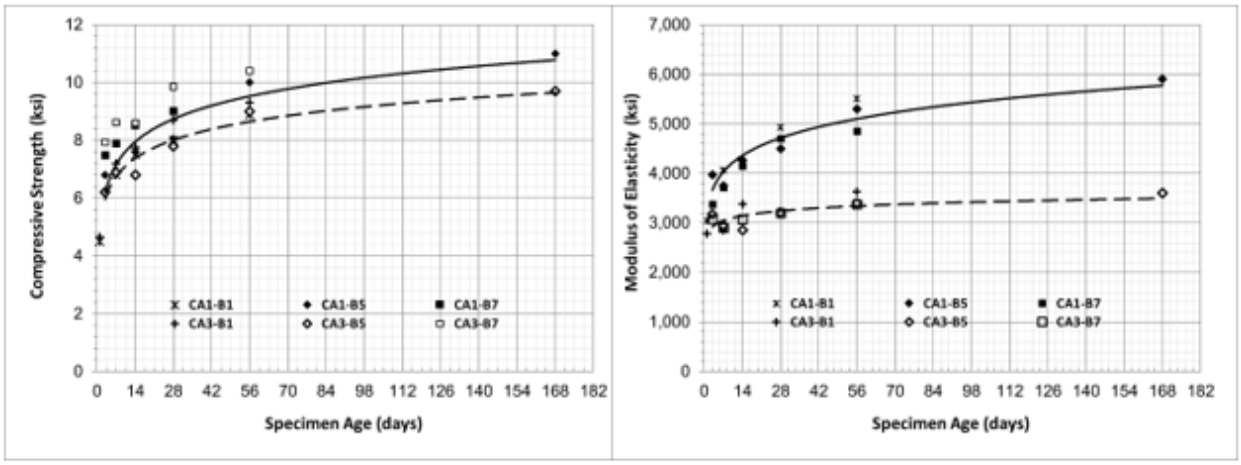

(a) (b)

Figure 7. Development of compressive strength and elastic modulus of HSRM and standard concrete: (a) compressive strength vs. specimen age and (b) modulus of elasticity vs. specimen age

Researchers observed that the plant-produced concrete batches had properties consistent with the concrete batches developed in the laboratory during the material development and qualification phase. The compressive strength developed as expected for both the HSRM and standard concrete, with the HSRM concrete exhibiting a compressive strength comparable to the standard concrete. However, the modulus of elasticity for the HSRM concrete appeared to plateau after its early strength was achieved, while the modulus of elasticity for the standard concrete continued to increase over time. The modulus reduction achieved by both plant batches was approximately 35 percent at 58 days and 40 percent at 168 days. Figure 8 shows the correlation between the modulus of elasticity and compressive strength of the HSRM and standard concrete materials for the plant-produced batches.

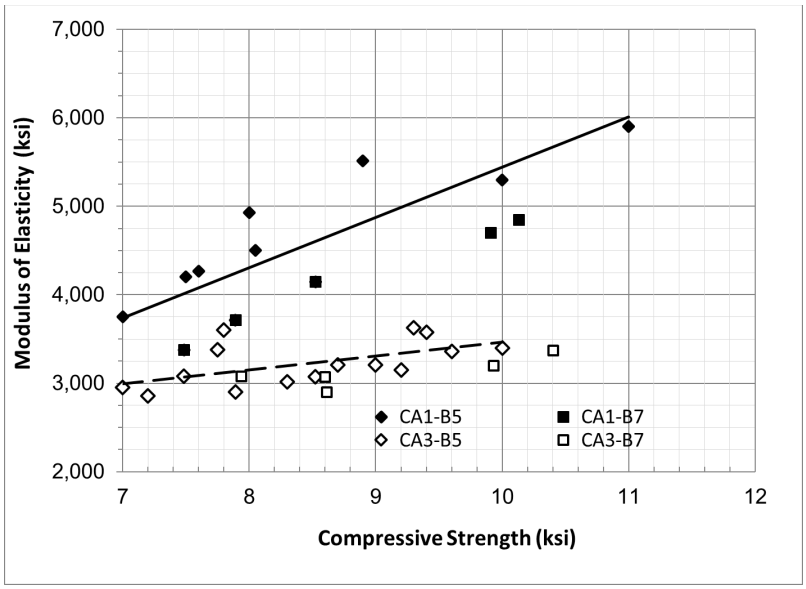

Figure 8. Correlation of modulus of elasticity with compressive strength for the HSRM and standard concrete

4.2 Tie Qualification Tests

Qualification testing of the standard and HSRM ties followed the test procedures set forth in the AREMA Manual for Railway Engineering, Chapter 30 – Ties, Part 4.9.1.1 a-f, and 4.9.1.2 a, b.. Five HSRM ties and five standard ties were tested in the Structures Laboratory at USC. Testing per AREMA 4.9.1.2 was conducted by RailTEC at UIUC on two HSRM and two standard ties. The average compressive strength at the time of testing of the CA1-B5 and CA3-B5 concrete was 9.9 ksi and 9.8 ksi, respectively. The average modulus of elasticity of the standard concrete CA1-B5 was 5,300 ksi, and of the CA3-B5 HSRM 3,400 ksi, representing an average reduction of 36 percent.

All HSRM and standard ties passed the AREMA qualification tests. However, one of the standard ties marginally passed the "Rail Seat A" positive loading test. A crack was detected in this tie when loads reached the design load level.

5. Laboratory Setup and Instrumentation

This section presents the test setup and the instrumentation for tests conducted at USC laboratories. In addition, it introduces the 3-dimensional, vision-based data acquisition system for digital image correlation (DIC) used for the full-field deformation, surface strain measurements, and crack detection.

5.1 Reaction Frame

All load testing was conducted in a reaction frame. The actuator was a 110-kips MTS with a 6-inch stroke. The actuator was also equipped with a load cell and LVDT. All tests were carried out in load control mode. The reaction frame is shown in Figure 9.

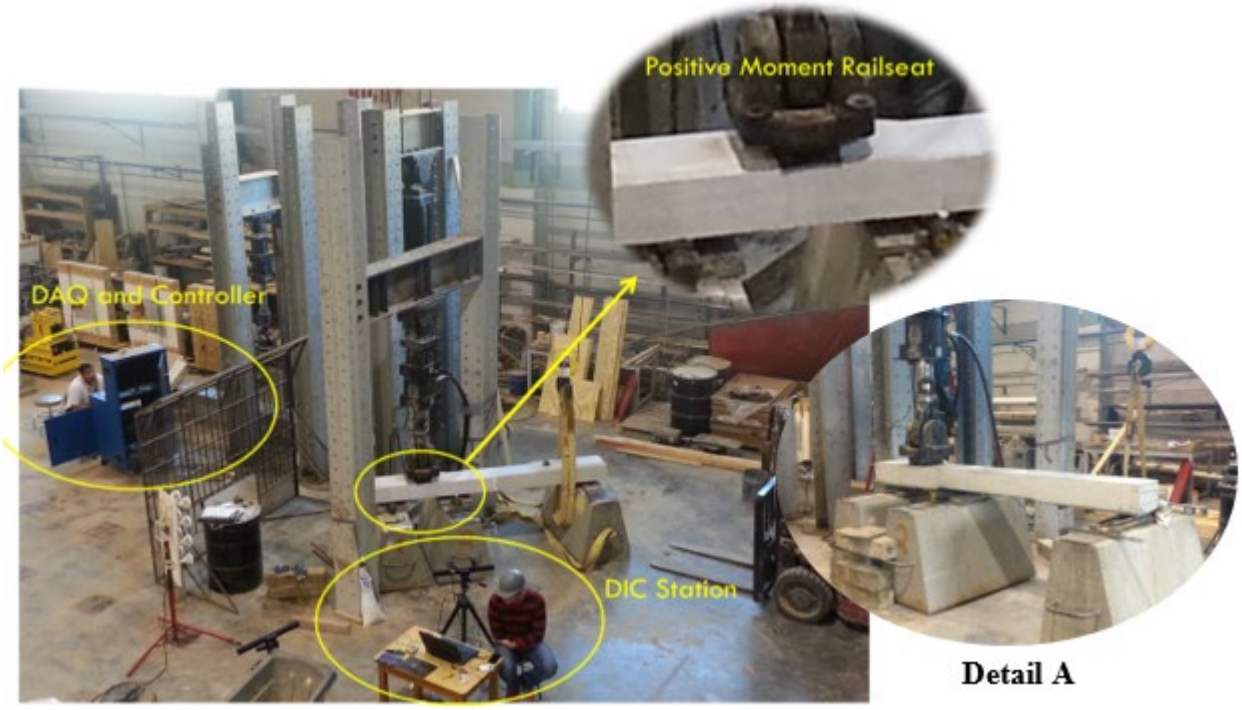

Figure 9. The reaction frame used for all load tests

5.2 Indoor Track Testing Facility

In addition to the reaction frame tests, the ties were tested under simulated track conditions in the full-scale indoor track load testing facility. Figure 10 shows the track panel configuration.

Figure 10. Indoor railway track testing facility

5.3 Instrumentation

Conventional measurement devices were employed for all tests. Specifically, linear voltage differential transformers (LVDTs) were used to measure the deflections at discrete locations on the specimen and to measure strand slippage. For deflection measurements, the LVDTs were secured to a single 2- by 4-foot wood board at predetermined spacing with their tips in contact with the surface of the tie. For strand slippage measurements, the LVDT was clamped to the specimen and the tip was in contact with the exposed strand face Strain gages, specifically designed for use on concrete elements, were also attached to the surface of the tie.

5.4 Vision-Based, Full-Field Measurements

Digital image correlation (DIC) is a unique suite of non-contacting, vision-based, full-field measurement methods developed over the past 3 decades (Luo, Chao, Sutton, & Peters, 1993; Luo, Chao, & Sutton, 1994) (Sutton, Orteu, & Schreier, 2009; Sutton, 2013). The DIC methods can be used for large and extremely small specimens. Measurements using both 2-dimensional and 3-dimensional DIC have been successfully made for a wide range of materials, loading, and temperature conditions. In addition to deformation measurements, the method can detect crack development and propagation and damage evolution. The following sections present the DIC system and one validation study used in this work. Details on the data acquisition and image processing procedures and additional verification and application studies of the DIC system used in this work have been published in the literature (Rajan et al., 2017; Sutton, et al., 2017).

5.4.1 Imaging System and Components

. The stereo DIC system used in this research consisted of a pair of cameras and lenses, low-heat-emission lighting, a computer for image acquisition, cables, calibration tablets, speckle application kits, and VIC-3D® software, as shown in Figure 11.

Figure 11. Stereo vision system components

5.4.2 DIC Validation Study

To verify the consistency among the measurements taken by the different instrumentation, a validation study was conducted. To this end, a four-point bending test of the standard concrete tie for center binding loading was completed. The specimen was loaded to 20 kips, and the load was applied in 2-kip increments. The load rate was set to 5 kips per minute, and the load was held for 1 minute at each increment. The test setup is shown in Figure 12. The instrumentation consisted of:

(a) One strain gage installed at the midspan and two strain gages installed at 15 inches on each side of the midspan and at the tension side of the tie, as shown in Figure 12.

(b) One LVDT installed at the midspan and two LVDTs installed at 15 inches on each side of the midspan at the tension side of the tie.

(c) StereoDIC imaging of the side of the tie to compute the deformation and strain fields during testing. At each load hold, images were acquired and correlated to the images of the unloaded specimen.

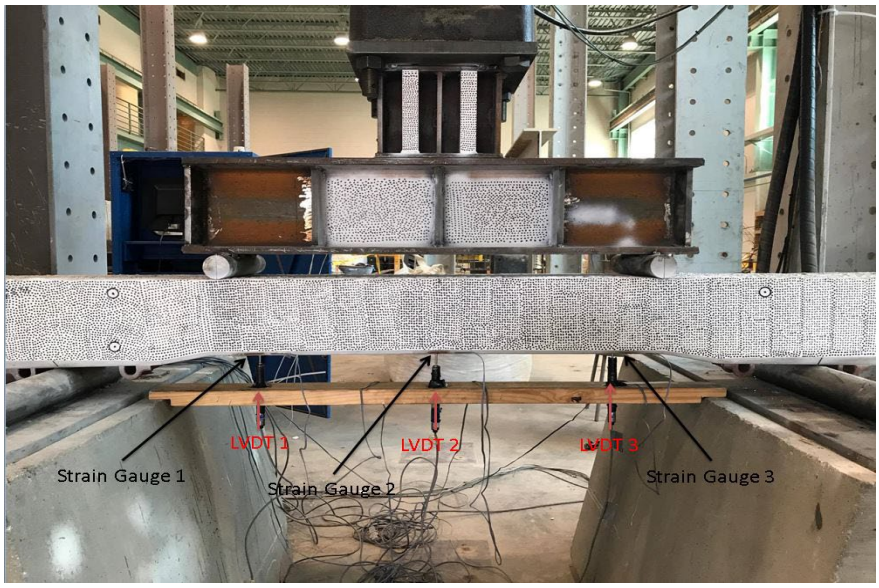

Figure 12. Test setup for the validation study of the DIC data acquisition approach

Figure 13 shows the longitudinal strain profile at the midspan cross-section of the prestressed concrete tie as computed from DIC measurements for load levels of 14, 18, and 20 kips. The horizontal axis shows the longitudinal strain, and the vertical axis shows the location along the depth of the tie. Strain gage measurements were acquired at a single point on the tension surface of the tie. Figure 13 also shows the strain gage measurements as dots at about -85 mm on the y-axis. Note that the DIC computed strain field extended from +70 mm to -70 mm along the cross-section and did not capture the strain values at the location of the strain gages. It was evident, however, that when the strain profile lines computed by the DIC were extrapolated to the location of the strain gages, the DIC measurements and strain gage measurements were in excellent agreement.

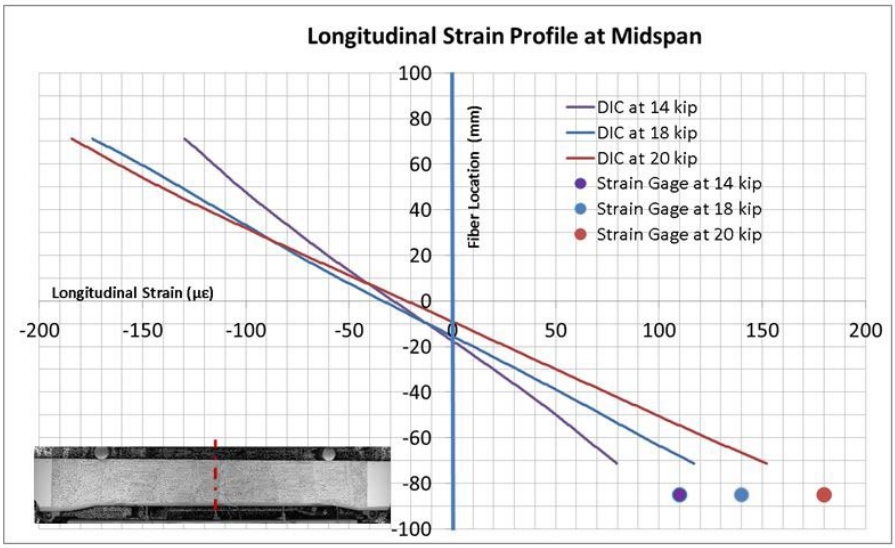

Figure 13. Longitudinal strain profile along a cross-section at the midspan of the prestressed concrete tie

Figure 14 shows the longitudinal strain at the location of the strain gages as acquired by the strain gage at different loads. There is excellent agreement between the longitudinal strain value as computed by the DIC system and extrapolated to the location of the strain gage.

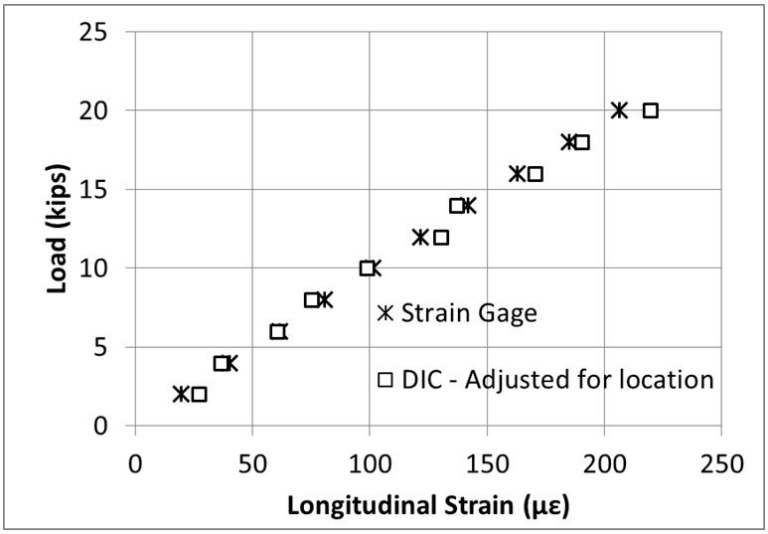

Figure 14. Load vs. longitudinal strain at the extreme tension fiber at the midspan as acquired by strain gages and the StereoDIC system

The last comparison study in this report pertains to the load-deflection response at the midspan of the tie as measured by the LVDT and the DIC system when the tie was loaded beyond the first cracking to approximately 70 kips. Figure 15 shows the load deflection response where the excellent agreement between the two data acquisition systems was evident. The DIC data acquisition system was superior to the conventional LVDT and strain gage systems by far, since it captured the full strain fields and identified crack size and location on the surface of the specimen monitored, as demonstrated in Figure 16.

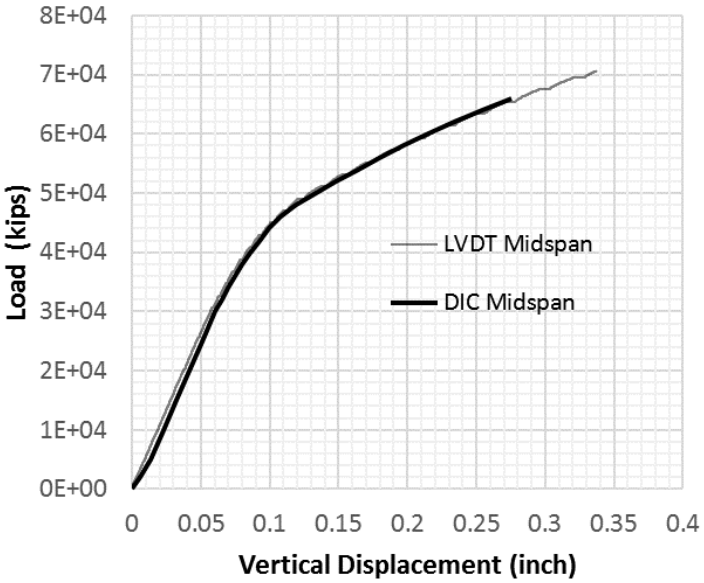

Figure 15. Load vs. vertical deflection at the midspan as acquired by LVDTs and the StereoDIC system

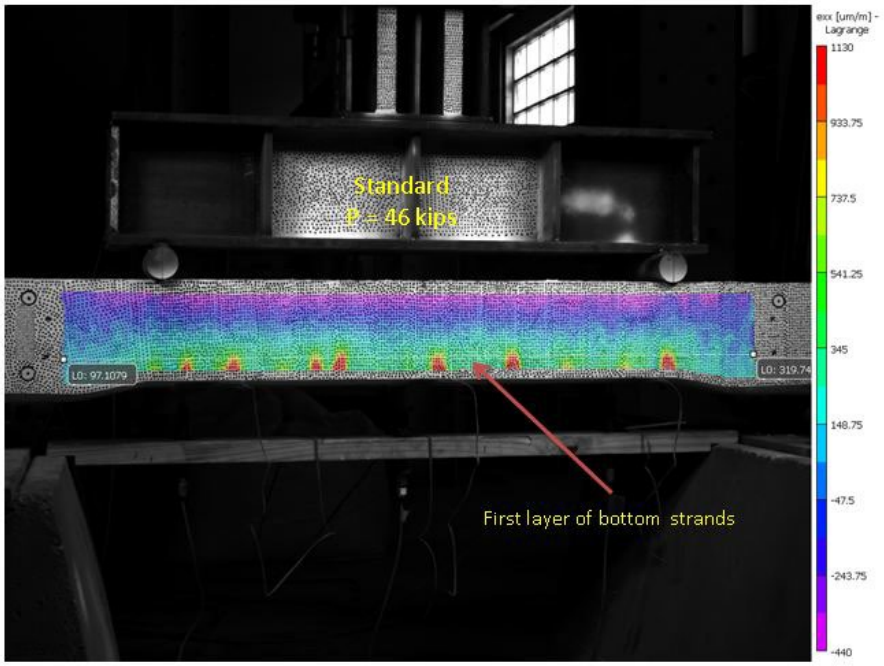

Figure 16. Color map showing the longitudinal strain field on the surface of the standard tie under 46-kip load. Cracks that extend to the first layer of strands are evident.

6. Performance Assessment

This section presents a comparative study on the performance of the HSRM and standard ties under service and ultimate loads and various support conditions and demonstrates the benefits of HSRM concrete in prestressed ties. These studies were based on both experimental investigations and parametric investigations through computer simulations. The experimental investigations were largely based on the testing program at the University of South Carolina and details on the test setups are available in Abdulqader (2017). The computer simulations were based on finite element analysis (FEA). The development, calibration, verification, and validation of the associated FEA models, as well as the parametric studies, are available in Zeitouni (2017). The following sections discuss three areas that demonstrate the benefits of using HSRM in concrete ties, i.e., load to first cracking, amplitude and gradient of the stress and strain fields, and ultimate load capacity as observed in rail seat loading tests and loading under center binding conditions.

6.1 Rail Seat Flexure Performance

The experimental setup was as indicated in AREMA qualification tests Chapter 30, section 4.9.1.4 (AREMA, 2013) and is shown in Figure 17. Three HSRM ties and three standard ties were tested in positive moment configuration and loaded to failure. The average load to first cracking of the HSRM ties was 10 percent higher than the design load, while the average load to first cracking of the standard tie was 1 percent higher than the design load. At the design load, the longitudinal strain fields were captured by the StereoDIC system and typical fields are also shown in Figure 17 in the form of color maps superimposed on the side of the ties.

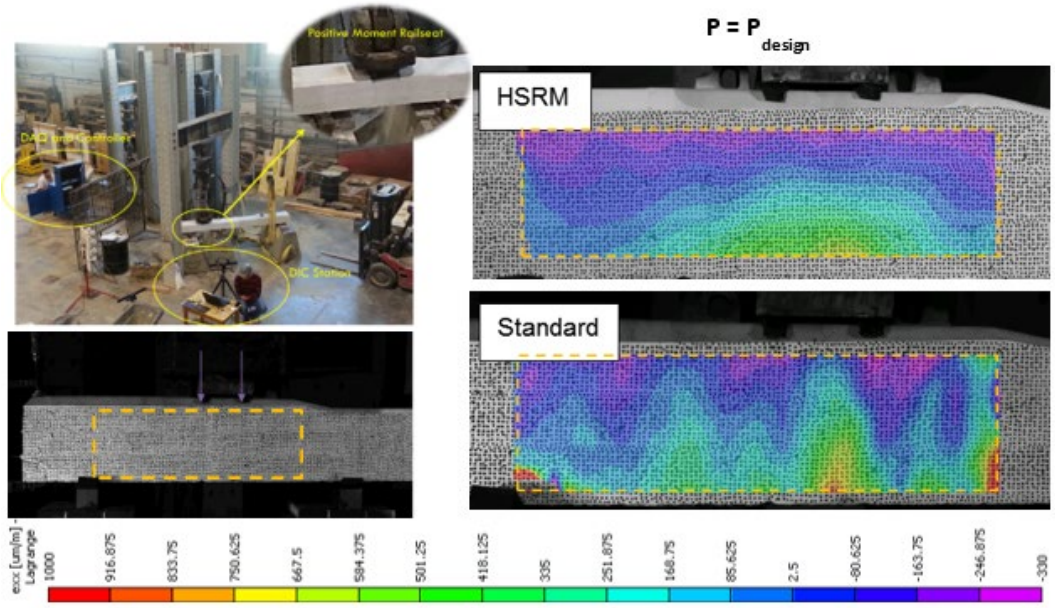

Figure 17. Rail seat positive moment testing

The damage evolution in each tie is particularly interesting. Researchers observed that the HSRM concrete yielded a smoother strain gradient than the standard concrete. Loading continued until failure of the ties. The average value of the ultimate load of the standard tie was 92 kips (180 percent of the design load). The ultimate load to failure in two of the three HSRM

ties exceeded the 105-kip capacity of the actuator, while the third tie failed at 97 kips, representing failure at least at 200 percent of the design load.

Similar observations were made at load levels of 127 percent and 175 percent of the design load. Figure 18 shows the longitudinal strain field as a color map superimposed on the side of the ties at the two loading levels for a representative standard and HSRM tie. At 127 percent of the loading, a very distinct crack formed on the standard tie that extended to the first line of strands, while there was evidence that a second crack had started to form. At 175 percent of the loading, the standard tie exhibited two very distinct and deep cracks that approached the second line of strands, indicating imminent failure. However, HSRM ties at 175 percent of the design load exhibited a third crack that never appeared in the standard tie. Note that this third crack appeared at approximately 160 percent of the design load. All three cracks were shallower compared to the standard tie and did not reach the second line of strands at this loading level. Note that similar behavior was observed for rail seat loading for negative moments.

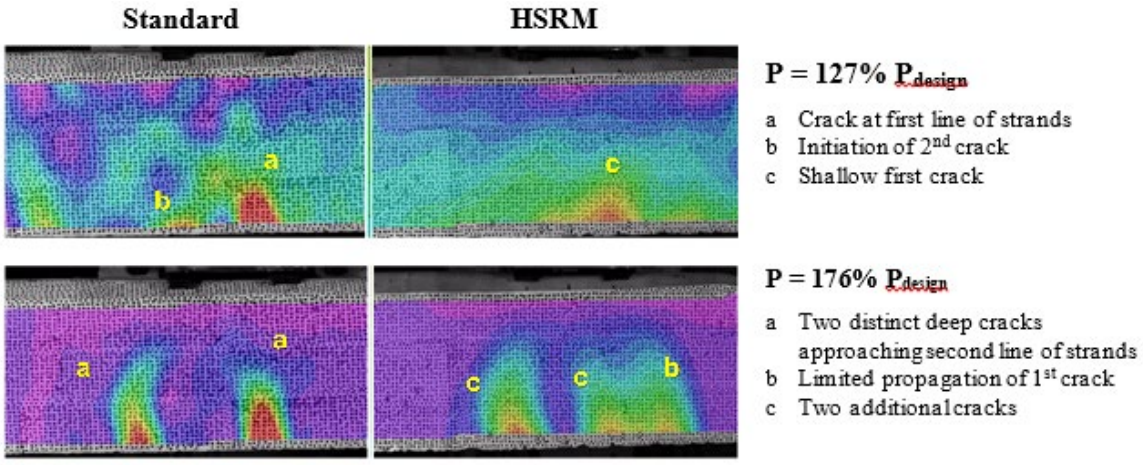

Figure 18. Cracking at 127% and 176% of the design load for the standard and HSRM ties

6.2 Mid-Tie Flexure Performance

Among the most critical issues affecting the performance of concrete ties is cracking of the tie from center binding (Zeman, Edwards, Barkan, & Lange, 2009). Tensile stresses on the top surface of the tie are not effectively redistributed in the tie due its high rigidity. In this section, the performance of the HSRM ties is evaluated through laboratory testing under monotonic and cyclic loading.

6.2.1 Monotonic Loading and Pure Moment Conditions

A 4-point bending test, demonstrated the benefits of using the lower rigidity HSRM concrete (Abdulqader, 2017). The test was a modification of the AREMA standard test, Section 4.9.1.6, Center Negative Bending Moment Test (AREMA, 2013). To create a wider shear-free region on the tie, loading was applied through a spreader beam with the loading points spaced 34 inches apart. The testing configuration is shown in Figure 20.

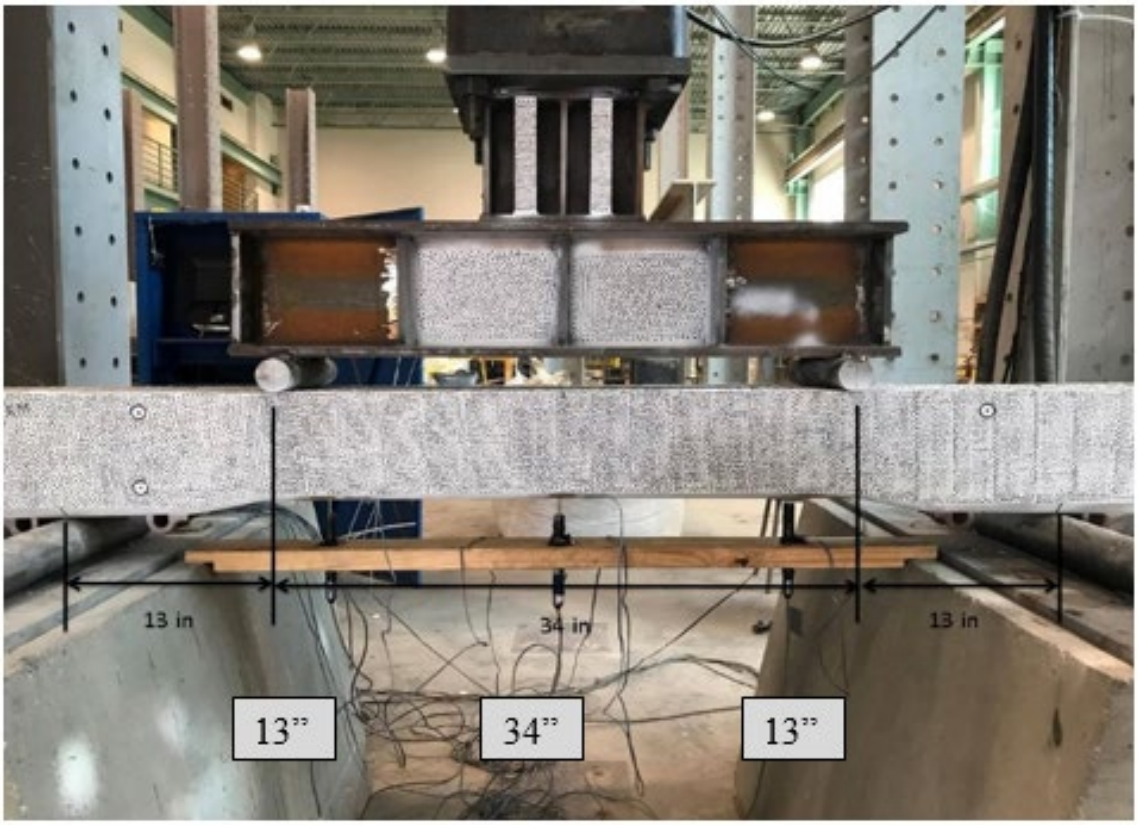

Figure 19. Test setup for the modified 4-point center negative moment test.

The total load required to create the center negative design moment in the modified 4-point bending was computed as P_{design} = 32 kips. The tie was loaded to failure, and the load was recorded when: (a) the first crack appeared, (b) the crack reached the first line of strands, and (c) the tie failed. Table 5 shows the recorded values as a percentage of the design load, $\%P_{design}$. The nominal value of the load in kips is also shown in parentheses. The cracking maps, as captured by the DIC system, are shown in Figure 21 for three load levels. Note that the HSRM tie exhibited a higher number of cracks that were not equally spaced compared to the standard tie. This was a strong indication of stress redistribution after first cracking.

Table 5. Modified 4-point bending load at characteristic damage levels

	First Crack $\%P_{design}$ (kips)	Crack to 1st Strand $\%P_{design}$ (kips)	Ultimate $\%P_{design}$ (kips)
Standard Tie	131 (42)	143 (46)	250 (80)
HSRM Tie	137 (44)	156 (50)	263 (84)
Difference	6 (2)	13 (4)	13 (4)

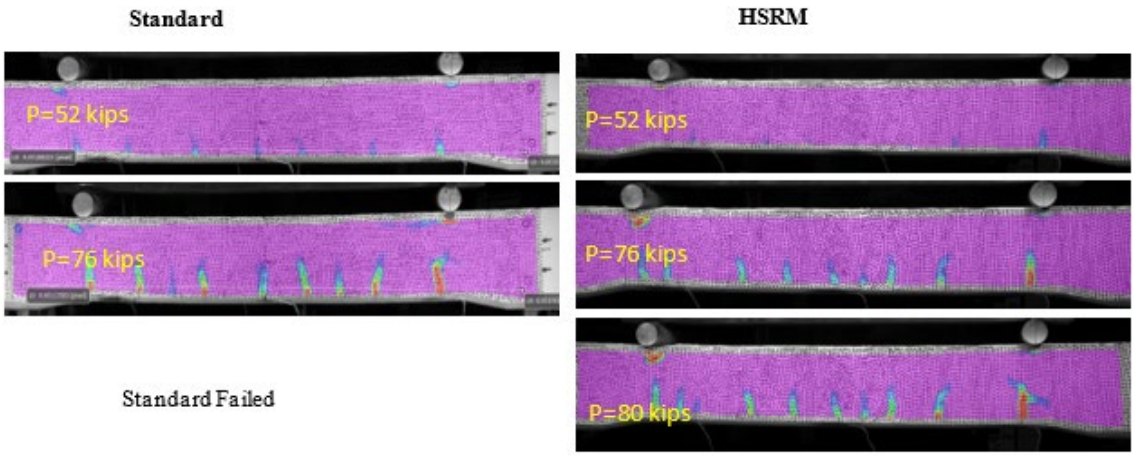

Figure 20. Cracking maps as of the standard and HSRM ties during loading

6.2.2 Cyclic Loading

The fatigue behavior of prestressed concrete ties under center binding support condition has long been a subject of interest, yet only limited research has been reported in the literature. The load carrying capacity and fatigue behavior of prestressed concrete ties under cyclic loads were experimentally investigated by means of a 4-point, midspan negative bending test. The ties were supported to prevented lateral and longitudinal movement during the loading cycles. Figure 23 shows the test setup.

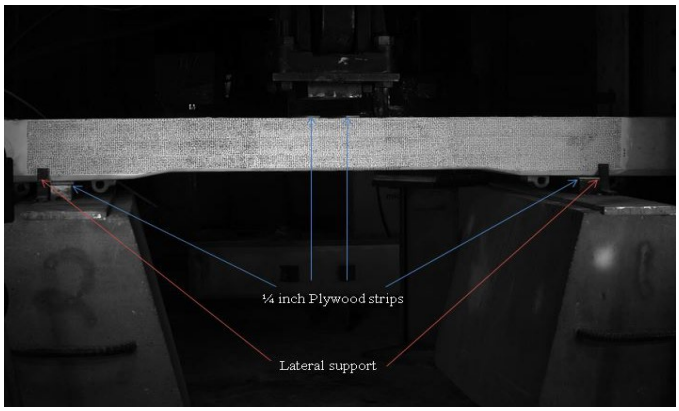

Figure 21. Test setup for cyclic loading test under center binding conditions

The AREMA manual does not provide any guidelines for such a test. USC developed the following test procedure:

Fatigue Testing Procedure

Stage 1: Three million load cycles were applied. The load range was 2 kips to 13.5 kips and corresponded to 90 percent of the load that would develop the design moment at midspan. The load was applied at a frequency of 2 cycles per second. The load cycling was paused every 48 hours (approximately 350,000 cycles), and a monotonic static test was performed from 2 kips to 13.5 kips. During the static test, the side surface of the ties was imaged at loads 2, 6, 8, 10, 12, and 13.3 kips for full-field DIC deformation measurements. After the image acquisition, the

cyclic testing resumed. Once the 3 million load cycles were reached, the tie was loaded until a crack reached the first level of strands. At this point the load was recorded.

Stage 2: Cyclic loading was then restarted as in Stage 1 but the load was applied in the range of 2 kips to 16.5 kips. The upper limit corresponded to 110 percent of the load associated to the design moment. As in Stage 1, the cyclic loading was paused every 48 hours, the tie was loaded monotonically to 16.5 kips, and images were acquired at load levels 2, 4, 6, 8, 10, 12, 13.5, 15, and 16.5 kips for DIC full-field deformation measurements. The cyclic loading continued until an additional 3 million cycles were applied, for a total of 6 million cycles.

Stage 3: The tie was loaded monotonically until failure, and the full-field deformation measurements were captured at load levels 0, 2, 6, 8, 10, 12, 13.5, 15, 16.5, 18, 20, 22.5, 27, 29, 31, and 33 kips. If failure did not occur, the load was increased manually by 1 kip until failure.

Results

Stage 1

The strain field did not show any significant changes during the first 3 million load. All strain in the HSRM tie remained in the range -400 $\mu\varepsilon$ to 440 $\mu\varepsilon$ when the tie was loaded to 90 percent of the design load (13.5 kips). The maximum deflection at the midspan was $0.046 \pm 8\text{x}10^{-4}$ inches. No cracking was detected through visual inspection or the DIC measurements. Figure 24 (a) shows the strain field color map superimposed on the side of the tie between the rail seats when the tie was loaded statically with 13.5 kips force after $1.177\text{x}10^6$, $2.027\ \text{x}10^6$, $2.745\ \text{x}10^6$, and $3\text{x}10^6$ load cycles. The standard tie showed similar behavior, as expected. The maximum deflection at the midspan was $0.031 \pm 5\text{x}10^{-4}$ inches. It is evident that the HSRM tie is about 48 percent more flexible than the standard tie which is consistent with the reduction of modulus of elasticity of the HSRM concrete. Figure 24 (b) and (c) show the corresponding elastic curve between the supports for the HSRM and standard tie.

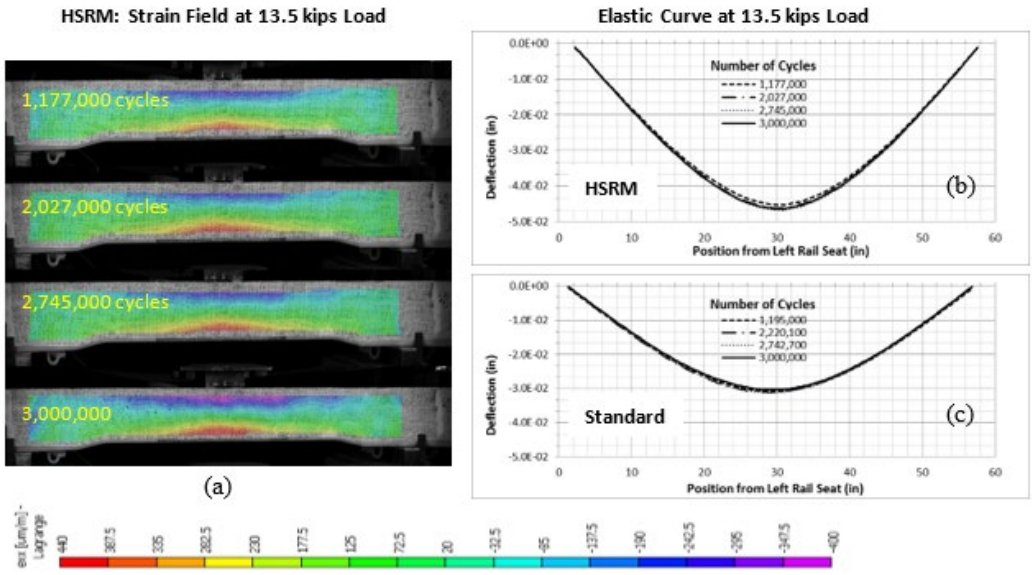

Figure 22. Static tests of the HSRM tie after 13.5 kip load cycles: (a) longitudinal strain ε_{xx} field color maps; (b) HSRM tie elastic curves between supports; and (c) standard tie elastic curves between supports

After 3 million load cycles, the ties were loaded until a crack reached the first line of strands. The corresponding loads were 19 kips for the standard tie and 20 kips for the HSRM tie, and the associated strain fields are shown in Figure 25.

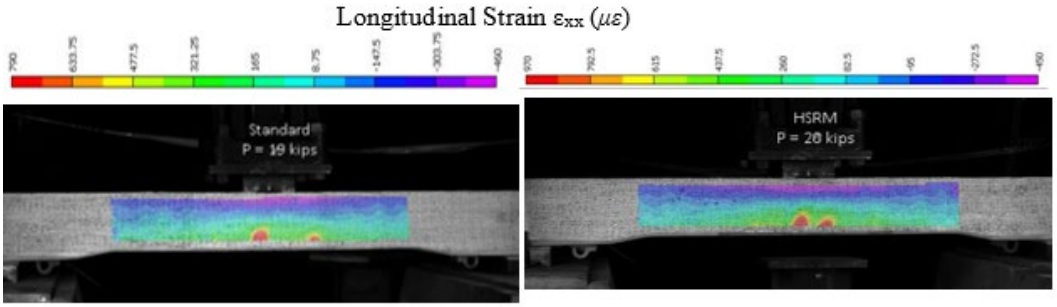

Figure 23. Longitudinal strain field ε_{xx} when the crack reaches the first line of strands in the standard tie at load 19 kips (left) and HSRM tie at load 20 kips (right).

Stage 2

Both ties were subjected to an additional 3 million cycles. The strain field did not change significantly. All strain in the HSRM tie remains in the range -420 $\mu\varepsilon$ to 460 $\mu\varepsilon$ when the tie was loaded to 90 percent of the design load (13.5kips) and in the range -510 $\mu\varepsilon$ to 715 $\mu\varepsilon$ when the tie was loaded to 110 percent of the design load (16.5 kips). The maximum deflection at the midspan was $0.0676 \pm 1\text{x}10^{-4}$ at 110 percent of the design load. No additional cracking was detected. Furthermore, the pre-existing cracks did not propagate. Figure 26 (a) shows the strain field color map superimposed on the side of the tie between the rail seats when the tie was loaded statically with 16.5 kips force after $0.848\text{x}10^6$, $1.348\ \text{x}10^6$, $2.174\ \text{x}10^6$, and $3\text{x}10^6$ load cycles in the range 0–16.5 kips. The standard tie showed similar behavior, as expected. The maximum deflection at the midspan was $0.043 \pm 6\text{x}10^{-4}$ inches. In this case the HSRM tie is approximately 57 percent more flexible than the standard tie. Figure 26 (b) and (c) show the corresponding elastic curve between the supports for the HSRM and standard tie.

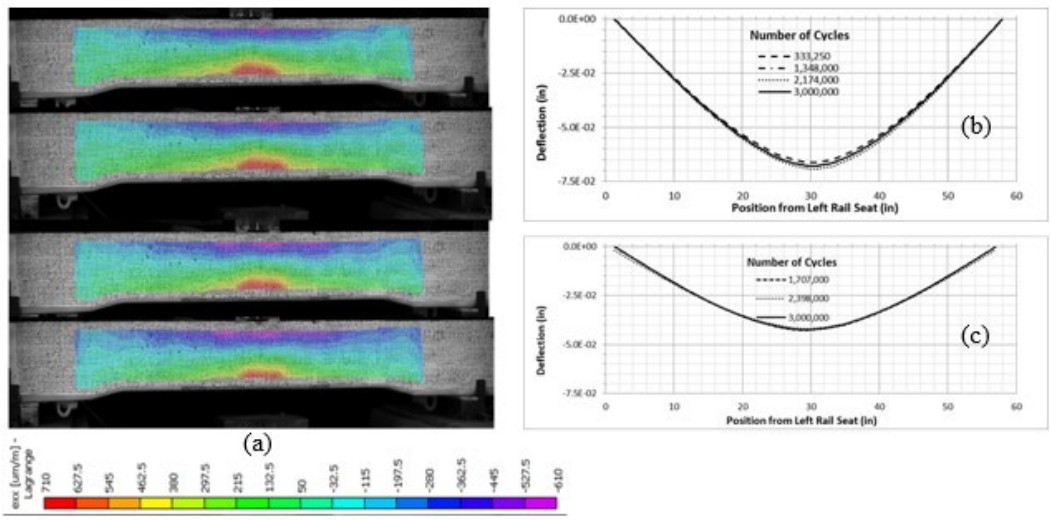

Figure 24. Static tests of the HSRM tie under 16.5-kips load after predetermined number of cycles during Stage 2 of cyclic loading: (a) longitudinal strain ε_{xx} field color maps; (b) HSRM tie elastic curves between supports; (c) standard tie elastic curves between supports

Stage 3

At the end of the 6 million cycles, both ties were loaded to failure. The ultimate load that caused the HSRM tie to fail (collapse) was 35 kips, while the standard tie collapsed at 33 kips. Figure 27 shows the load-deflection curve at a point, P, between the loading points, as indicated in the inset of Figure 27. The linear elastic stiffnesses for the HSRM and standard ties were estimated at 338 kips/in and 441 kips/in, respectively, representing a 30 percent difference.

Figure 28 shows the formation and progression of cracks as the load increased. The HSRM ties better distributed the load, as evidenced by the more regularized strain field around and between the cracks, in contrast to the standard ties, where the cracks were very distinct and were longer at the same load level.

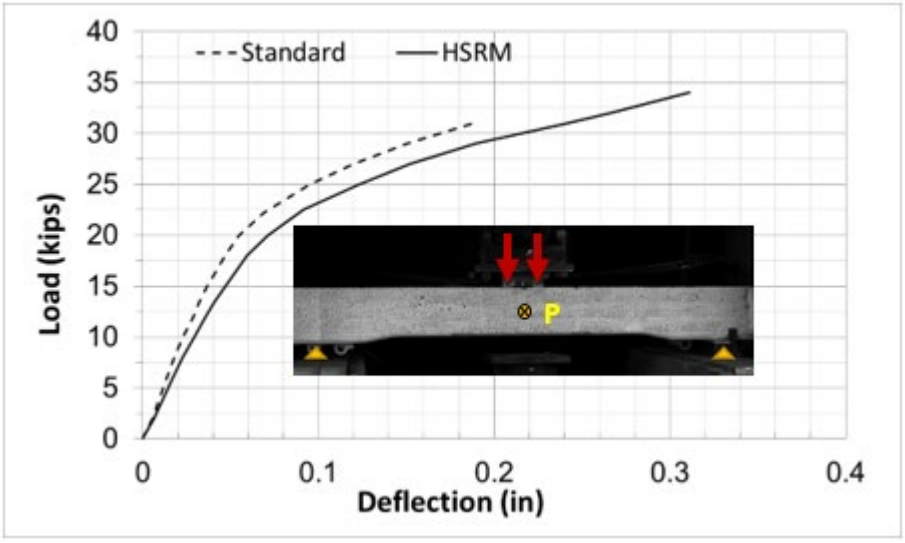

Figure 25. Load-deflection for ultimate load test

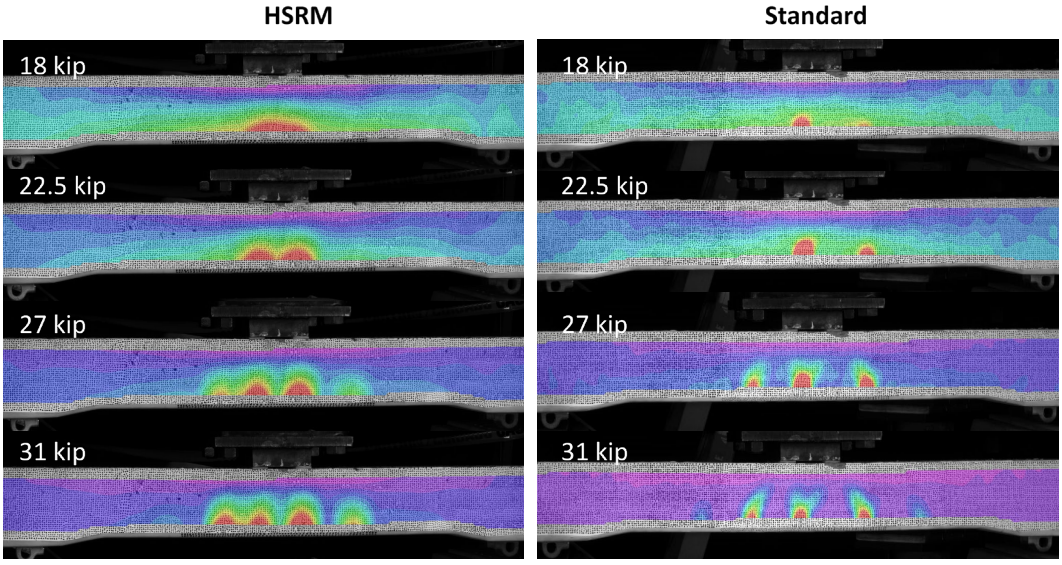

Figure 26. Longitudinal strain field during testing to failure after 6 million load cycles shown for the HSRM ties (left column) and standard ties (right column).

6.3 Loading under Simulated Track Support Conditions

The performance of the HSRM and standard ties under simulated track support conditions was compared using laboratory tests and computer simulations.

6.3.1 Laboratory Testing

Laboratory testing under simulated track support conditions was carried out by RailTEC at the Research and Innovation Laboratory (RAIL) at the Harry Schnabel, Jr. Geotechnical Laboratory in Champaign, Illinois. This section presents a summary of the tests and findings as reported by RailTEC (2016). Ties were tested using a loading frame, shown in Figure 29, where both rail seats were loaded simultaneously in the vertical direction. Ties were tested under two support conditions: full support and center-binding. To simulate these different support conditions, rubber pads were used. The pads chosen were 1 inch (25.4 mm) thick and 1 foot (305 mm) long and wide. The pads had a hardness of 50 Shore A durometer. To simulate full support, they were placed under the entire length of the tie, and to simulate severe center-binding, they were placed under the center 4 feet of the tie. The tests were executed according to the static-load testing procedure developed by RailTEC at UIUC (Bastos, Dersch, & Edwards, 2015). The test plan was designed to produce strains, bending moments, vertical deflection, and center-cracking under a given rail seat load. To accomplish this, strain gauges and potentiometers were used.

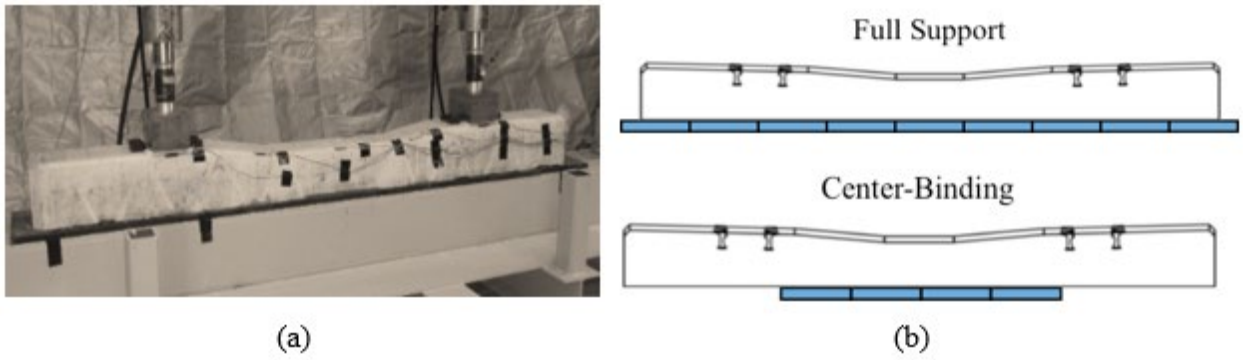

Figure 27. Loading frame, test setup, and support conditions for loading under simulated track support conditions in the laboratory

Six strain gauges were used on each tie: one at each rail seat, one at each intermediate location between the rail seats and center, and two at the center. Tie sides were marked as side A and side B, with the strain gauge numbering running from side A to side B. Fifteen potentiometers were used for measuring vertical displacements and quantifying tie shape under loading. Supported by a separate frame, the potentiometers were placed along the top of the tie at even spacing. They were similarly numbered 1 to 15, running from side A to side B. The strain gage and potentiometer location are depicted in Figure 30 and Figure 31, respectively.

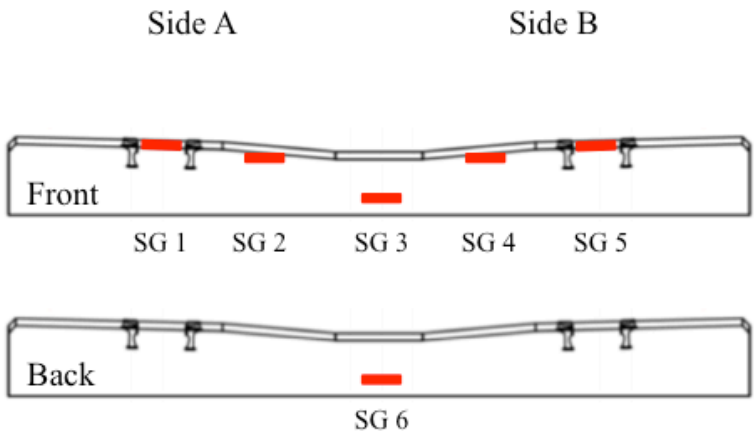

SG 1 and 5 are on the crosstie chamfer at the rail seat center
SG 2 and 4 are immediately below the chamfer at 15 inches away from the midspan
SG 3 and 6 are on the crosstie midspan at 1 inch above the crosstie bottom

Figure 28. Strain gage locations

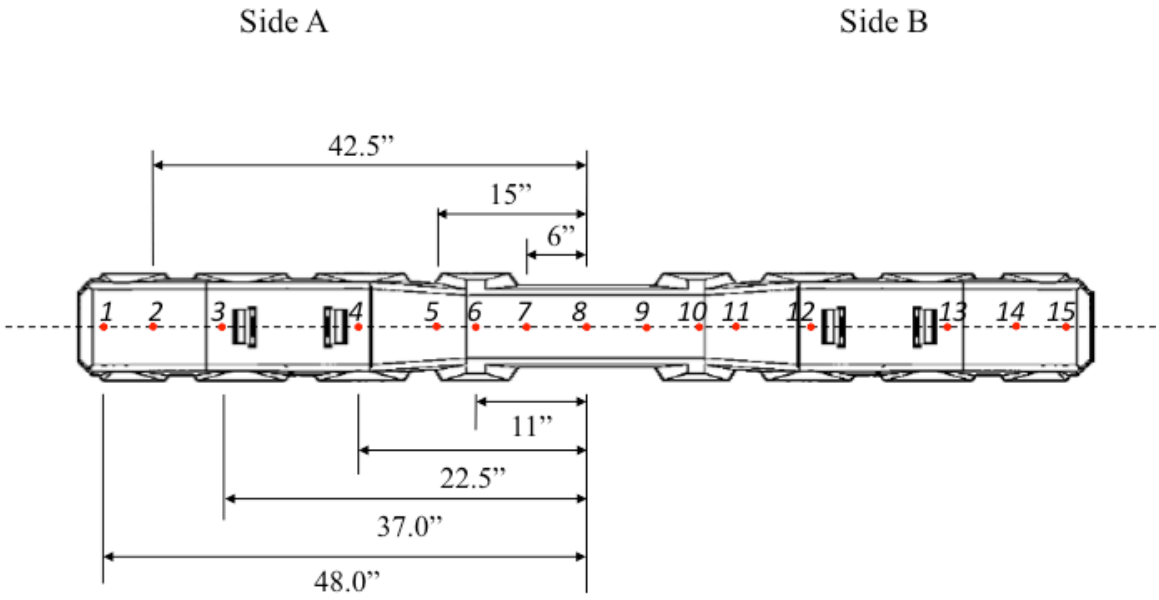

Figure 29. Potentiometer locations

For each tie, the full-support case was tested first, with data recorded from 0- to 20-kip loads at each rail seat. The center-bound case was then tested in the same manner. During center-binding tests, marks of all crack locations were made on the tie while it was subjected to a 20-kip rail seat load.

Strain

Strain gauge data were collected and compared across tie types and support conditions using box and whisker plots (Figure 32). In all cases, the rail seat load was 20 kips on both rail seats. The

diamonds in the box plots represent the mean strain for each case, and horizontal lines inside each box represent the median strain. In the full support condition, the rail seats experienced strains roughly in the range of -100 $\mu\varepsilon$ to -200 $\mu\varepsilon$. The negative sign indicates a compressive strain, consistent with the positive bending expected at the rail seats. In the severe center-binding condition, however, they experienced virtually no strain, as one would expect based on Euler-Bernoulli beam theory. This trend applied to both standard and HSRM ties. The effect on the center strain gauges was the opposite of that on the rail seats, as expected. The center of the tie experienced very little strain under the full support condition, and typical strains of -400 $\mu\varepsilon$ to -600 $\mu\varepsilon$ under center-binding.

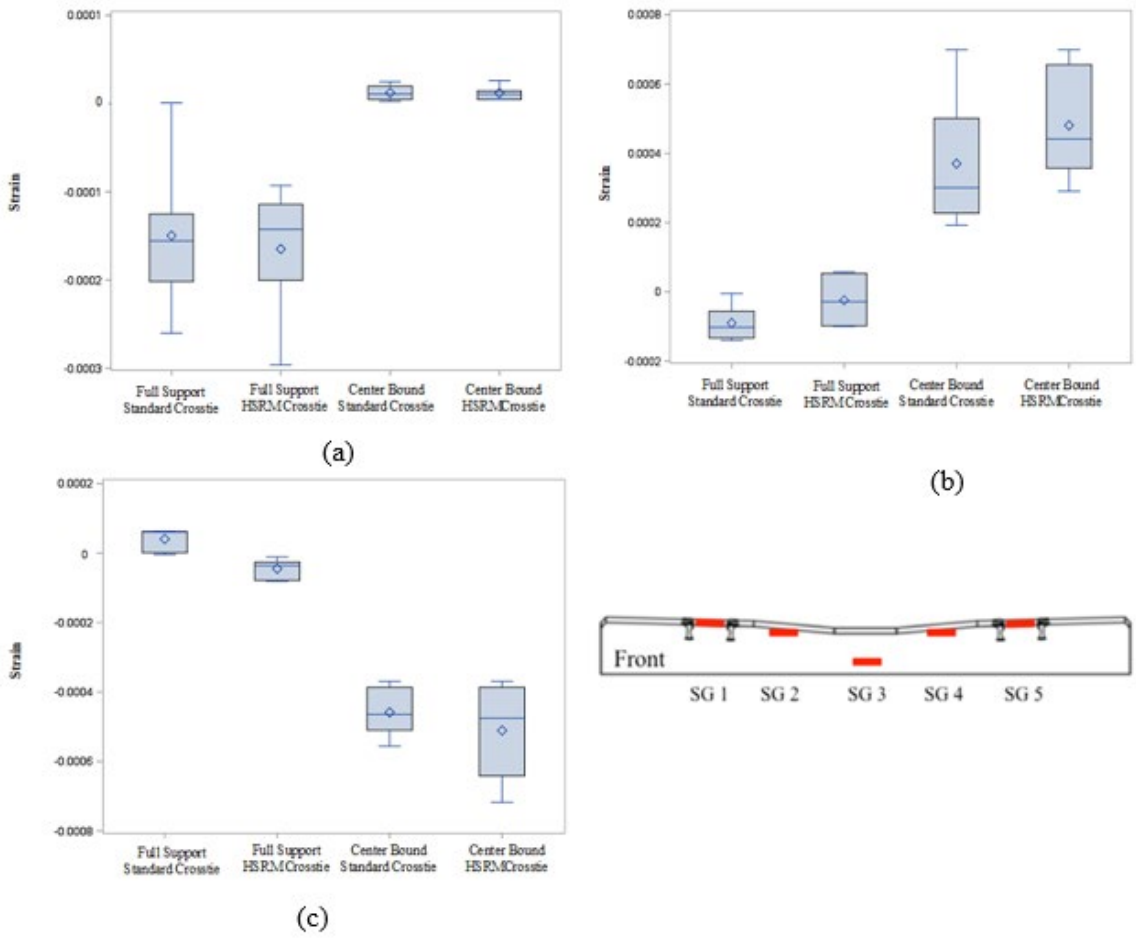

Figure 30. Strain gauge results: (a) rail seat strain gauges; (b) intermediate strain gauges; and (c) center strain gauges

By looking at the box plots, the difference between the strains of standard and HSRM ties was not clear. A statistical model was developed to aid in the analysis. This model was adapted from prior work and incorporated the concept of completely randomized design with two factors (Ott & Longnecker, 2008).

The effects of support condition and crosstie type (Standard or HSRM) were determined to be either significant or insignificant based on a two-way analysis of variance (ANOVA). The ANOVA results show that support condition is significant at any reasonable confidence level. Although the effects of the crosstie type showed significant difference between the standard and

HSRM crossties at an 85 percent confidence level, there is not enough evidence to assess the effects of the crosstie type at 90 percent confidence level. Increasing the number of tested crossties would help to increase the confidence level.

Bending Moments

Bending moments were calculated for each of the 6 gauges in each of the 12 tests. Data points taken from identical tie types and locations were then averaged (that is, six data points per average, excepting the standard tie rail seat data, which had five data points due to the existence of a bad strain gauge on rail seat A of tie 1) to give the results shown in Table 6.

Table 6. Averaged bending moment results (unit: kip-inches)

Tie Type	Support Type	Railseat *kip-in*	Intermediate *kip-in*	Center *kip-in*
Standard Tie	Full Support	168	62	27
	Center-Bound	-14	-255	-309
HSRM Tie	Full Support	136	17	-26
	Center-Bound	-9	-307	-306

The results showed that the standard and HSRM ties behaved similarly under loading. In the center-bound case, the standard ties had an average center bending moment of -309 kip-in and the HSRM ties had a center bending moment of -306 kip-in. HSRM ties tended to have greater intermediate negative bending moments than their standard counterparts for the center-binding support condition. This observation indicated a smoother load distribution in the HSRM ties and led to the introduction of the modified 4-point bending test designed at USC and discussed in Section 6.2.1. In the full support condition, the standard ties exhibited a positive bending moment at the bottom of the tie, indicating positive center bending.

Vertical Displacements

The vertical displacement data taken from the potentiometers were averaged for each tie type for each support case, as well as for each side of the tie (that is, six test data points went into each average value, except for the center). The graphs of these data are in Figure 33. Average deflection at 20 kips represent the shape of the tie under loading. In the full support case, there was very little overall displacement in any part of the tie. The HSRM ties deflected the most at the ends of the tie, with the average displacement there being 0.0833 inch. Unexpectedly, the standard ties actually underwent positive center-bending, and thus their maximum average displacement in the full support condition was at the center. The deflection here was on average 0.061 inch, while at the ends of the tie it was only 0.054 inch. This agreed with the bending moment results presented in the preceding section. In the center-bound support condition, deflections were much greater, particularly at the ends of the ties. Standard ties deflected on average 0.314 inch at the ends, and HSRM ties 0.334 inch at the ends. Note that the deflections of the HSRM and standard ties were very similar for the center-bound conditions when the material remained in the linear elastic range, i.e. no damage had taken place. This observation

was consistent with the deflections obtained from the modified 4-point bending tests, as discussed in Section 6.2.1 and shown in Figure 22.

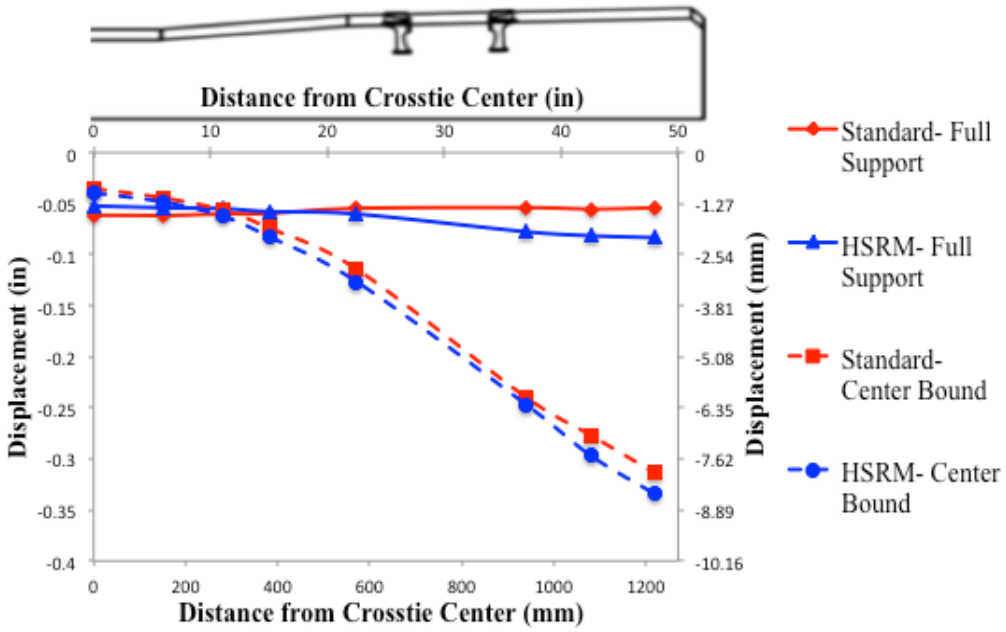

Figure 31. Average deflection at 20 kips

Cracking

A qualitative analysis of the crack patterns produced after loading under the center-bound support condition showed that the standard ties had fewer cracks that formed across the entire width, while the HSRM ties exhibited more, shorter cracks that did not extend through the width of the tie. Typical cracked HSRM and standard ties are shown in Figure 34. These observations were consistent with the findings of the modified 4-point bending tests discussed in Section 6.2.1.

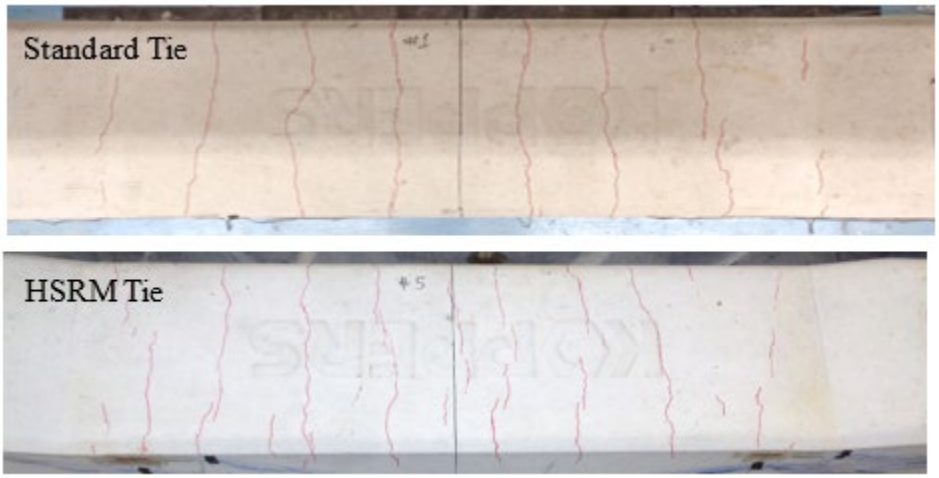

Figure 32. Typical cracking pattern after center binding of standard (top) and HSRM (bottom) ties

6.3.2 Parametric Studies through Computer Simulations

The parametric studies for the simulated track support condition were conducted based on FEA. Detailed non-linear material models of the ties and the development, validation, and verification of the tie models have been presented in Zeitouni (2017) and Zeitouni, Rizos, and Qian (2018). The FEA model was developed in ABAQUS and considered the prestressing strand action explicitly in a separate analysis step. The damaged plasticity model was adopted for modeling the concrete, and cohesion elements were used for modeling the concrete-strand bond. Additional information about these constitutive models is available in Zeitouni (2017). Three concrete materials were considered – the standard concrete and two HSRM concretes with modulus reductions of 23 percent and 40 percent. These values represented a typical reduction range observed in the course of this work. The concrete material properties are listed in Table 7.

Table 7. Concrete material properties for the FEA analysis

Concrete Type	f'_c	E_c	f'_t	ν
Standard	8,618.25 psi (59.42 Mpa)	4,996,307.85 psi (34,448.33 Mpa)	948.55 psi (6.54 Mpa)	0.2
HSRM 22.6% Reduction	8,618.25 psi (59.42 Mpa)	3,868,156.5 psi (26,670.0 Mpa)	948.55 psi (6.54 Mpa)	0.2
HSRM 40% Reduction	8,618.25 psi (59.42 Mpa)	2,997,785.0 psi (20,669.0 Mpa)	948.55 psi (6.54 Mpa)	0.2

Three distinct support conditions were considered in this study. The three supports were selected to simulate a concrete tie that was fully supported beneath, at its two ends, and at its middle region by the ballast. Each rail seat was loaded with a vertical (V) load up to 40 kips, yielding a total vertical load of 80 kips. To account for trains moving on a curved track, a second load case was considered where a lateral (L) load equal to 12 kips was applied on one rail seat toward the field side. Thus, ratios of L/V=0.0 and L/V=0.6 were considered. The three models are shown in Figure 35. For each combination of boundary conditions, concrete material, and L/V ratio, the longitudinal stress (S_{33}), von Mises stress, and tensile damage were measured throughout the tie and recorded for each simulation.

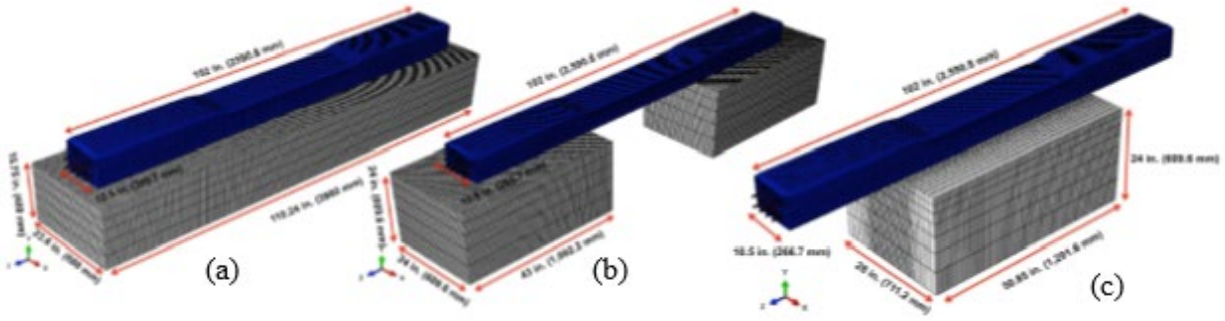

Figure 33. Three different ballast support condition representing: (a) full support (new track condition), (b) loss of center support, and (c) loss of rail seat support

In all support and load cases, the HSRM exhibited stress amplitude reduction and a smoother distribution of the stress field.

The support conditions shown in Figure 35 (a) and (b) did not produce any damage in the tie for all materials and all L/V ratios, and the tie response remained linear elastic. However, the center-binding condition shown in Figure 35 (c), caused the response of the tie to become nonlinear before the axle load was reached, and cracking started to form on the top surface of the ties.

Figure 36 shows the damage progression, where it was verified that crack initiation occurred at higher loads (39 kips on the standard and 43.8 kips for the HSRM tie) when HSRM concrete was used. The crack pattern was consistent with what had been observed in the laboratory, i.e., very distinct, width-wide cracks appeared in the standard tie as opposed to multiple shorter cracks on the HSRM tie.

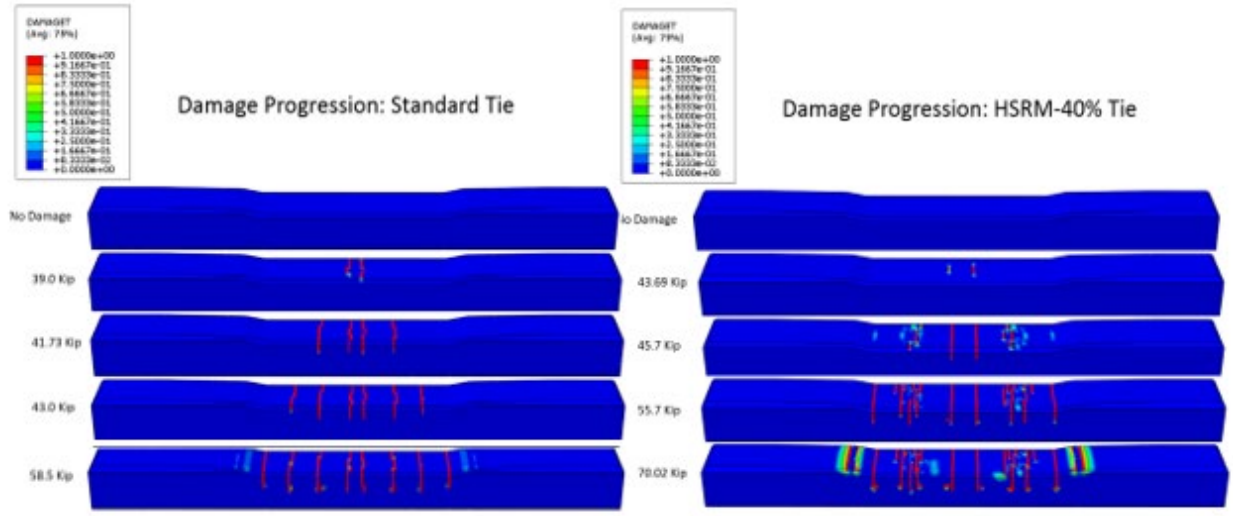

Figure 34. Damage progression for the standard tie (left) and the HSRM tie (right)

In all cases, however, the stresses were reduced when the 23 percent and the 40 percent HSRM concrete material was used. To quantify this reduction, the concrete tie was divided into three distinct regions to further compare the performance of each concrete tie. The three regions were defined as "End A," "End B," and the "Center" region. Within each region, locations of concern, such as sites where large stress amplitudes were observed or sites that were most prone to develop cracks under increasing loads, were recorded along the top and bottom surfaces of the concrete tie. The center region represented the midsection of the tie with a constant cross-section (middle 36 inches [914.4 mm]). End A depicted the region facing the field side, which contained the rail seat with the combination of vertical and lateral loads (if applicable). This region was 33 inches (838.2 mm) long and began at the tie end and terminated where the center region began. In contrast, End B represented the remaining 33 inches (838.2 mm) of the tie on the opposite side of the tie where only vertical loads were applied.

The two HSRM concrete ties considered in this study outperformed the standard concrete tie in all the load and support scenarios by better distributing the stresses throughout the tie. This effect was most pronounced in the center-binding support case, when the initiation of cracks appeared on the HSRM ties at higher loads as compared to the standard concrete ties. The HSRM-22.6 percent tie experienced its first crack approximately 2.84 kips and 1.36 kips after the standard concrete tie has already cracked for the L/V=0 and L/V=0.6 load cases. The HSRM-40 percent delayed the initiation of cracks by undergoing an additional 4.7 kips and 2.77 kips for the L/V=0 and L/V=0.6 load cases, when compared to the standard tie. Finite element simulations showed

that reducing the elastic modulus of the standard concrete by 40 percent could allow as high as 4.7 kips of additional load before the first crack was initiated. The positive behavior of the concrete ties was not just noticed in the nonlinear regions of the tie but also in the linear regions.

In the continuously supported and end supported simulations, the concrete ties remained in the linear region and no plastic strains were developed. Even in the linear region, it was obvious that the two HSRM material models showed favorable responses when compared to the standard tie. For the continuously supported tie, it was preferred for the concrete tie to have lower tensile and compressive stress in its middle, top, and bottom fibers. Both HSRM concrete ties exhibited this desired behavior. As compared to the standard tie, the HSRM-22.6 percent showed as high as an 11 percent increase in the compressive stress at the top fibers of the tie which were susceptible to tension cracking with increasing loads and as high as a 4.83 percent reduction in the compressive stresses in the bottom fibers of the tie which would reach crushing with increasing loads. The HSRM-40 percent showed as high as a 20.37 percent increase in the compressive stress at the top fibers of the tie (moving further from a tensile state) and as high as a 9.48 percent reduction in the compressive stresses in the bottom fibers of the tie, when compared to the standard tie.

For the end supported ties, it was preferred for the concrete tie to have lower tensile stresses in the bottom fibers of the tie and lower compressive stresses in the top fibers of the tie. Again, both HSRM ties exhibited this desired behavior. The HSRM-22.6 percent tie showed as high as a 6.67 percent reduction in the compressive stresses at the top fibers and as high as a 77.8 percent increase in the compressive stresses at the bottom fibers (moving further from a tensile state), when compared to the standard tie. The HSRM-40 percent tie showed as high as a 12.95 percent reduction in the compressive stresses at the top fibers while delaying the development of pure tensile stresses at the bottom fibers of the concrete, thus preventing cracking when compared to the standard tie.

The percent reduction is summarized in Table 8. Researchers observed that the stress reduction was higher for the more resilient concrete, HSRM-40 percent. Note that the values shown for the standard tie were the nominal recorded stress values. Researchers also noted that stress reduction was achieved in all support and load combinations and that the maximum benefits of over 50 percent stress reduction were realized for the case of center-binding conditions on a tangent track. The detailed FEM analysis is presented in Zeitouni (2017).

Table 8. Summary of stress reduction for all concrete materials, support conditions and L/V ratios. Standard concrete shows nominal stress values in ksi. HSRM ties show the stress reduction as a percentage of the stress in the standard tie.

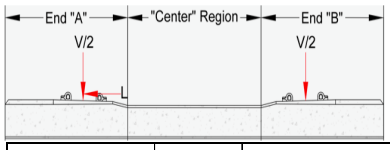			Longitudinal Stress, S33 (Mpa)					
			Continuous Support		End Supports		Center Support	
			L/V = 0 (V = 80^k)	L/V = 0.6 (V = 80^k)	L/V = 0 (V = 80^k)	L/V = 0.6 (V = 80^k)	L/V = 0 (V = 36^k)	L/V = 0.6 (V = 28^k)
HSRM-22.6%	Top	End A	2%	1%	7%	1%	1%	1%
		Center	5%	11%	7%	6%	26%	15%
		End B	2%	2%	7%	4%	1%	1%
	Bottom	End A	4%	2%	11%	2%	Center Governs	Center Governs
		Center	4%	5%	10%	24%	7%	4%
		End B	4%	13%	11%	78%	Center Governs	Center Governs
HSRM-40%	Top	End A	4%	2%	13%	2%	2%	1%
		Center	9%	20%	13%	12%	52%	30%
		End B	4%	4%	13%	8%	2%	2%
	Bottom	End A	10%	4%	19%	2%	Center Governs	Center Governs
		Center	8%	9%	18%	45%	14%	9%
		End B	10%	26%	19%	149%	Center Governs	Center Governs
Standard	Top	End A	-18.7	-20.2	-20.0	-18.6	-6.55	-6.85
		Center	-5.79	-4.10	-17.1	-22.9	5.13	4.92
		End B	-18.7	-19.1	-20.0	-20.3	-6.55	-6.38
	Bottom	End A	-4.81	-3.10	-3.92	-13.2	Center Governs	Center Governs
		Center	-16.5	-15.9	-7.02	-3.04	-26.2	-25.9
		End B	-4.81	-1.72	-3.92	-0.763	Center Governs	Center Governs

6.3.3 In-Track Testing

The objective of this series of tests was to assess the performance of the HSRM ties under simulated in-track conditions. Testing was performed in the Indoor Track Testing Facility discussed in Section 4.2, and the track was symmetrically loaded by a 110-kip MTS actuator through a spreader beam. Two different track configurations were tested. Both track panels were 16 feet long and contained nine ties spaced 20 inches on-center. RE132 rail was installed with e-clip fasteners. The first case considered a standard track, consisting of the standard ties. The second track was an HSRM track consisting of HSRM. The testing procedure for both tracks consisted of cyclic loading of the track and monotonic loading of the loaded tie.

The first series of tests involved cyclic load testing of the tracks to investigate the in-track performance of each tie type and was similar to the procedure discussed in Section 6.2.2, where cyclic load-testing was performed in three stages:

Stage 1: Three million load cycles were applied. The load ranged from 2 kips to 36 kips. This load corresponded to 90 percent of the load that would cause initial damage under center-binding conditions. The load was applied at a frequency of up to 3.5 cycles per second. Once the 3

million load cycles were reached, the loaded tie was removed from the track and loaded in a modified 4-point bending configuration (Section 6.2.1) until a crack reached the first level of strands. DIC was used to map a full 3-dimensional strain field of the tie during this loading. At this point the load was recorded.

Stage 2: Cyclic loading was then restarted as in Stage 1 and to the same load range of 10 kips to 36 kips. The cyclic loading continued until an additional 3 million cycles were applied, for a total of 6 million cycles.

Stage 3: The loaded tie was removed from the track and was loaded in a modified 4-point bending configuration (Section 6.2.1) until failure. The full field deformation measurements and failure load were captured.

Table 9 shows the load required to induce first crack, and for the crack to reach the first line of strands during the 4-point bending test at the end of Stage 1, and the load required to fail the tie, at the end of Stage 3. Researchers noted that the capacities of the ties after cyclic loading in the testing track was consistent with the tests in Section 6.2.1.

Table 9. Modified 4-point bending load after 3 and 6 million load cycles

	First Crack (stage 2) $\%P_{design}$ (kips)	Crack to 1st Strand (stage 2) $\%P_{design}$ (kips)	Ultimate (stage 3) $\%P_{design}$ (kips)
Standard Tie	131 (42)	159 (51)	280 (90)
HSRM Tie	144 (46)	172 (55)	312 (100)
Difference	13 (4)	13 (4)	32 (10)

7. Conclusion

This report presents the development of a HSRM concrete and its benefits in prestressed concrete railroad ties. The use of weathered granites as aggregates in higher strength concretes has consistently produced a resilient concrete material that has a modulus of elasticity significantly lower (up to 50 percent) than standard concretes that contain limestone coarse aggregates. In this work the weathered granite was used as a direct substitute of the limestone aggregate used in a current design without any further modifications to the concrete mix or the tie design. The experimental investigations and the computer simulations presented in this report quantify the benefits of using the HSRM-resilient concrete in prestressed concrete railroad ties. The following conclusions are noted:

- The HSRM concrete compressive strength was comparable to the standard mix.
- The HSRM modulus of elasticity was lower than the standard mix, by as much as 50 percent.
- HSRM concrete had a much higher abrasion resistance than the standard concrete.
- HSRM ties met the AREMA performance requirements and equaled or exceeded the performance of the standard ties.
- HSRM ties exhibited smoother stress gradients and exhibited stress redistribution after initial cracking.
- HSRM ties have lower stress amplitudes compared to standard ties under the same loads
- HSRM ties withstood higher ultimate loads.
- The use of weathered granites to produce the HSRM concrete ties did not impact the production process or increase the cost of the ties.

The use of HSRM represents a technology-based modification in concrete tie technology that improves the safety of rail service and maintenance operations without impacting fabrication cost and processes. Note that additional benefits may be gained if the tie were redesigned to take advantage of the HSRM material properties. This is a topic for future investigations. This study suggests that the HSRM concrete may be a cost-effective alternative concrete to the traditional high-performance concrete used in prestressed concrete ties with the potential to increase the service life of the tie.

8. References

Abdulqader, A. (2017). *Product Qualification and Performance Assessment of HSRM Prestressed Concrete Railroad Ties Through Laboratory Testing* (MS thesis). https://scholarcommons.sc.edu/etd/4545/. University of South Carolina, Columbia, SC.

ACI. (2014). ACI 318-14 Building Code Requirements for Structural Concrete (318-14) and Commentary (318R-14). American Concrete Institute.

ACI Committee 363. (1992). ACI 363R-92 State of the Art Report on High Strength Concrete. ACI Committee 363. American Concrete Institute

Aitkin, P., & Mehta, P. (1990). Effect of Coarse-Aggregate Characteristics on Mechanical Properties of High-Strength Concrete. *ACI Materials Journal, 87*, 103–107.

Alexander, M.G., & Milne, T.I. (1995). Influence of Cement Blend and Aggregate Type om Stress-Strain Behavior and Elastic Modulus of Concrete. *ACI Materials Journal, 92*, 227–235.

AREMA. (2013). *Manual for Railway Engineering.* Lanham, MD: American Railway Engineering and Maintenance-of-Way Association.

Bastos, J., Dersch, M., & Edwards, J.R. (2015). Determination of Critical Track Conditions and Their Impact on the Performance of Concrete Crossties and Fastening Systems. *The Arema 2015 Annual COnference.* Minneapolis: AREMA.

BSCP. (1972). CP110: Parts 2&3 Use of Concrete. *British Standard Code of Practice*.

Giaccio, G., Rocco, C., Violini, D., Zappitelli, J., & Zerbino, R. (1992). High Strength Concretes Incorporating Different Coarse Aggregates. *ACI Materials Journal, 89*, 242–246.

Goodspeed, C.H., Venikar, S., & Cook, R.A. (1996). High-Performance Concrete Defined for Highway Structures. *Concrete International, 18*(2), 62–67.

Jeong, D., & Yu, H. (2012). Overview of FRA/Volpe Research on Concrete Ties. *International Concrete Crossitie & Fastning System Symposium.* Urbana-Champaign: U. of Illinois at Urbana-Champaign.

Kaewunruen, S., & Remennikov, A. M. (2010). Dynamic Crack Propagations in Prestressed Concrete Sleepers in Railway Track Systems Subjected to Severe Impact Loads. *Journal of Structural Engineering, 136*(6), 749–754.

Luo, P.F., Chao, Y.J., & Sutton, M.A. (1994). Application of Stereo Vision to 3-D Deformation Analysis in Fracture Mechanics. *Optical Engineering, 33*(3), 981–990.

Luo, P.F., Chao, Y.J., Sutton, M.A., & Peters, W.H. (1993). Accurate Measurements of Three-Dimensional Deformations in Deformable and Rigid Bodies Using Computer Vision. *Experimental Mechanics, 33*(2), 123–133.

Lutch, R.H., Harris, D.K., & Ahlborn, T.M. (2009). Prestressed Concrete Ties in North America. *AREMA Annual Conference.* Chicago: AREMA.

Manda, K.R., Dersch, M.S., Edwards, R.J., & Lange, D.A. (2014). Vertical Load Path Under Static and Dynamic Loads in Concrete Crosstie and Fastening Systems. *ASME/IEEE/ASCE Joint Rail Conference.* ASME. doi:10.1115/JRC2014-3832

Mayville, R.A., Jiang, L., & Sherman, M. (2014). *Performance Evaluation of Concrete Railroad Ties on the Northeast Corridor* [DOT/FRA/ORD-14/03] Washington, DC: U.S. Department of Transportation.

Ott, R., & Longnecker, M. (2008). *An Introduction to Statistical Methods and Data Analysis.* Boston: Cengage.

Peters, W.H., Ranson, W.F., Sutton, M.A., Chu, T.C., & Anderson, J. (1983). Application of Digital Image Correlation methods to rigid body mechanics. *Optical Engineering, 22*(6), 738–743.

Petrou, M. F., Rizos, D.C., Harries, K.A., & Hanson, J. (2004). Permeability of Portland Cement Concrete (PCC) Structures in South Carolina - Vol. II. *Final Report No ST04-04 to SCDOT/FHWA*.

RailTEC. (2016). High Strength Reduces Modulus (HSRM) Crosstie Testing at University of Illinois at Urbana-Champaign (UIUC). Report submitted to University of South Carolina, Dept. of Civil and Environmental Engineering.

RAILTEC. (2016). High Strength, Reduced Modulus (HSRM) Concrete Crosstie Testing at University of Illinois at Urbana-Champaign (UIUC). U. of South Carolina, Prepared for University of South Carolina.

Rajan, S., Sutton, M.A., Rizos, D C., Ortiz, A.R., Zeitouni, A.I., & Caicedo, J.M. (2017). A Steroo-Vision Deformation Measurement System for Transfer Length Estimates in Prestressed Concrete. *Experimental Mechanics*. doi:10.1007/s11340-017-0357-0

Sutton, M.A. (2013). Computer vision-based noncontacting deformation measurements in mechancs: A generational Transformation. *Applied Mechanics Review – Transactions of the ASME*.

Sutton, M.A., Matta, F., Rizos, D.C., Ghorbani, R., Rajan, S., Mollenhauer, D. H., . . . Lasprilla, A. O. (2017). Recent Progress in Digital Image Correlation: Background and Developments since the 2013 W.M. Murray Lecture. *Experimental Mechanics, 57*(1), 1–30. doi:10.1007/s11340-016-0233-3

Sutton, M. A., Orteu, J.J., & Schreier, H.W. (2009). *Image Correlation for Shaper, Motion and Deformation Measurements.* New York: Springer Publishing.

Van Dam, E. (2016). *Abrasion Resistance of Concrete and the Use of High Performance Concrete for Concrete Railway Crossties* (MS thesis). University of Illinois at Urbana-Champaign, Champaign, IL.

Van Dyk, B.J., Dersch, M.S., & Edwards, R.J. (2016). International Concrete Crosstie and Fastening System Survey – Final Results [RR 13-02]. Washington, DC: U.S. Department of Transportation.

Weart, W. (2008). Suppliers of railroad ties dedicate more resources to fulfill railroads' crosstie needs. *Progressive Railroading*.

Wu, Y., Ke-Ru, W., Bing, C., & Dong, Z. (2001). Effect of Coarse-Aggregate Characteristics on Mechanical Properties of High-Strength Concrete. *Cement and Concrete Research, 31,* 1421–1425.

Zeitouni, A. (2017). *Performance Assessment of HSRM Concrete Ties through Finite Element Model Simulations* (MS thesis). https://www.proquest.com/docview/2023509341?pq-origsite=gscholar&fromopenview=true. University of South Carolina, Columbia, SC.

Zeitouni, A., Rizos, D.C., & Qian, Y. (2018). Benefits of high strength reducued modulus (HSRM) concrete railroad ties under center binding support conditions. *Construction and Building Materials, 192*, 210–223.

Zeman, J. (2010). *Hydraulic Mechanisms of Conrete-Tie Rail Seat Deterioration* (MS thesis). University of Illinois at Urbana Champaign, Champaign, IL.

Zeman, J. C., Edwards, J. R., Barkan, C. L., & Lange, D. A. (2009). Failure Mode and Effect Analysis of Concrete Ties in North Americ. *9th International Heavy Haul Conference.* Shanghai.

ZETA-TECH. (2010). Assessment of Concrete Tie Life on US Freight Railroads. Fayetteville, GA: Railway Tie Association.

Abbreviations and Acronyms

HSRM	High Strength Reduced Modulus concrete
USC	University of South Carolina
SCDOT	South Carolina Department of Transportation
HPC	High Performance Concrete
L/V	Lateral to Vertical Load Ratio
DIC	Digital Image Correlation
StereoDIC	Stereoscopic Digital Image Correlation
DAQ	Data Acquisition
LVDT	Linear Variable Differential Transformer
FEA	Finite Element Analysis
HS	High Strength
A_{tr}	Area of tie at rail seat
A_{tc}	Area of tie at center
e	Strand eccentricity at rail seat
S_B	Section modulus wrt to bottom of tie
d_s	Strand diameter
A_s	Strand area
P_i	Prestressing force per strand
P_e	Effective force per strand
σ_i	Strand initial stress
σ_{ie}	Effective strand stress
N_s	Number of strands
P_{si}	Total prestressing force
P_{se}	Total effective force
E_s	Modulus of elasticity for steel
E_c	Modulus of elasticity of concrete
f_c'	Concrete compressive strength
f_t	Concrete tensile strength
ν	Poisson's ratio